

## Review

# ATP synthases: structure, function and evolution of unique energy converters

V. Müller<sup>a,\*</sup> and G. Grüber<sup>b,\*</sup>

<sup>a</sup> Department Biology I, Ludwig-Maximilians-Universität München, 80638 München (Germany),  
Fax: +49 89 2180 6127, e-mail: v.mueller@lrz.uni-muenchen.de

<sup>b</sup> FR 2.5-Biophysik, Universität des Saarlandes, 66421 Homburg (Germany), Fax: +49 6841 1626086,  
e-mail: ggrueber@med-rz.uni-saarland.de

Received 25 July 2002; received after revision 21 October 2002; accepted 22 October 2002

**Abstract.** A-, F- and V-adenosine 5'-triphosphatases (ATPases) consist of a mosaic of globular structural units which serve as functional units. These ion-translocating ATPases are thought to use a common mechanism to couple energy of ATP hydrolysis to ion transport and thus create an electrochemical ion gradient across the membrane. In vitro, all of these large protein complexes are able to use an ion gradient and the associated membrane potential to synthesize ATP. A-/F-/V-type ATPases are

composed of two distinct segments: a catalytic sector, A<sub>1</sub>/F<sub>1</sub>/V<sub>1</sub>, whose three-dimensional structural relationship will be reviewed, and the membrane-embedded sector, A<sub>o</sub>/F<sub>o</sub>/V<sub>o</sub>, which functions in ion conduction. Recent studies on the molecular biology of the A<sub>o</sub>/F<sub>o</sub>/V<sub>o</sub> domains revealed surprising findings about duplicated and triplicated versions of the proteolipid subunit and shed new light on the evolution of these ion pumps.

**Key words.** ATP synthase; archaea; methanogens; bacteria; eukarya; evolution; structure-function.

## Introduction

The ultimate goal of energy metabolism in living cells is the production of adenosine 5'-triphosphate (ATP) from ADP and inorganic phosphate. The majority of ATP in eukaryotes, most bacteria and the archaea is synthesized by the enzymes F<sub>1</sub>F<sub>o</sub>-ATP synthase (F-ATPase) and A<sub>1</sub>A<sub>o</sub>-ATP synthase (A-ATPase). The F-ATPase in its simplest, bacterial form is composed of 8 subunits ( $\alpha_3$ :  $\beta_3$ :  $\gamma$ :  $\delta$ :  $\epsilon$ :  $a$ :  $b_2$ :  $c_{9-14}$ ) compared with the more complex bovine heart mitochondrial F-ATPase, which consists of 16 subunits ( $\alpha_3$ :  $\beta_3$ :  $\gamma$ :  $\delta$ :  $\epsilon$ :  $a$ :  $b_2$ :  $c_{9-14}$ :  $d$ :  $e$ :  $f$ :  $g$ :  $A_6L$ :  $F_6$ :  $I$ : OSCP) (fig. 1) [1, 2]. The A-ATPase has at least 9 subunits ( $A_3$ :  $B_3$ :  $C$ :  $D$ :  $E$ :  $F$ :  $H$ :  $I$ :  $K_x$ ), but the actual subunit stoichiometry is unknown. In particular, the number of

proteolipid subunits in A<sub>1</sub>A<sub>o</sub>-ATPases is different in various organisms (12, 6 or 4) and a function of the number of the transmembrane helices in a given monomer (fig. 1, [3]). A 10<sup>th</sup> subunit (G) may be present. The F- and the A-ATPases transform energy from a gradient of ions across the membrane to synthesize ATP [4] and can reversibly link the equilibrium of ATP hydrolysis, catalyzed in the F<sub>1</sub>/A<sub>1</sub> domain, to the flux of cations (H<sup>+</sup> or Na<sup>+</sup>) through the membrane domain (F<sub>o</sub>/A<sub>o</sub>) [3] as in the genetically related vacuolar-type, V<sub>1</sub>V<sub>o</sub>-ATPases (V-ATPases). The V-ATPases, consisting of at least 13 distinct subunits ( $A_3$ :  $B_3$ :  $C$ :  $D$ :  $E$ :  $F$ :  $G_y$ :  $H_2$ :  $a$ :  $d$ :  $c$ :  $c'$ :  $c''$ ) (fig. 1), are required for a range of cellular processes including receptor-mediated endocytosis, renal acidification, bone reabsorption, neurotransmitter accumulation and activation of acid hydrolases [5]. The V-ATPase exhibits catalytic cooperativity similar to A- and F-type ATPase in ATP hy-

\* Corresponding author.

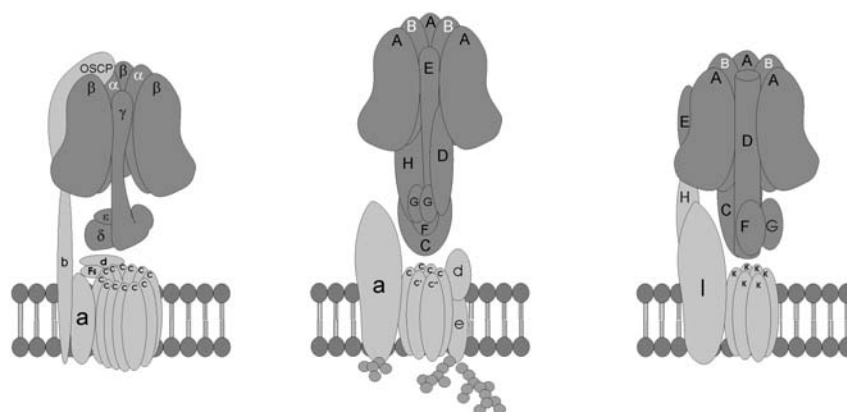


Figure 1. Model of the subunit arrangement in the bovine  $F_1F_0$ -ATPase (left),  $V_1V_0$ -ATPase from *Manduca sexta* (middle) and  $A_1A_0$ -ATPase from *Methanosarcina mazei* Gö1 (right).  $F_1/V_1/A_1$ - and  $F_0/V_0/A_0$ -subunits are labelled in dark and light gray, respectively. The dots indicate sugar residues. The subunit topology is based on molecular, biochemical and structural data [1, 3, 32, 78, 84, 85, 87]. Minor subunits (e, f, g,  $A_0L$ , I) of the  $F_0$  domain are not shown. The stoichiometry of the proteolipid subunits in  $A_1A_0$ -ATPase refers to the situation encountered in *Methanothermobacter thermautotrophicus* (16-kDa proteolipids).

drolysis [6–8]. However, in vivo, the enzyme is not involved in ATP synthesis but in vitro experiments have recently shown that it can also catalyze ATP synthesis [9]. Morphologically, the A-, F- and V-ATPases have three components (fig. 1): a membrane-bound domain,  $A_0/F_0/V_0$  that contains the ion channel, a connecting central stalk and an approximately spherical cytoplasmic domain,  $A_1/F_1/V_1$ , that contains the catalytic sites [1, 10, 11]. Side-view projections of the  $F_1F_0$ - [12, 13] and  $V_1V_0$ -ATPases [14, 15] showed a second stalk (stator) as a fourth distinct feature extending from the  $F_0$  or  $V_0$  portion. In the case of the *Escherichia coli*  $F_1F_0$  complex the central stalk is composed of  $\gamma_{ec}$  and  $\epsilon_{ec}$ , which is the equivalent of  $\delta_m$  in mitochondrial  $F_1F_0$ , and the stator is formed by the  $\delta_{ec}$  and  $b$  subunits (table 1) [16]. The bacterial  $\delta$  subunit ( $\delta_{ec}$ ) bears homology to one of the mitochondrial  $F_0$  subunits, called OSCP. The mitochondrial  $F_1$   $\epsilon$  subunit ( $\epsilon_m$ ) has no counterpart in the bacterial  $F_1F_0$  enzyme. The central element of the  $F_1$  complex, subunit  $\gamma$ , has been shown to move relative to the  $\alpha_3\beta_3$  complex during ATP hydrolysis. This rearrangement is proposed to drive the motion of a ring of  $c_{9-14}$  subunits in the  $F_0$  domain, each containing two transmembrane helices [17].

The ATPases arose from a common ancestor which underwent structural and functional changes leading to three distinct classes of enzymes present in three domains of life [3, 18]. The major subunits of A-type ATPases share about 50% sequence identity with V-type ATPases and about 25% sequence identity with F-type ATPases. The minor subunit composition is different, and those of V- and A-type ATPases are, in some cases, somewhat similar, but there is no obvious sequence similarity between the minor subunits of A/V-type and F-type ATPases, which probably reflects different functions, regulatory

Table 1. Listing of similar ATPase gene products in the three types of ATPases.

<i>Methanoarchaea</i> $A_1A_0$	<i>M. sexta</i> $V_1V_0$	Bovine $F_1F_0$
A	A	$\beta$
B	B	$\alpha$
C	C	—
—	D	—
D	E	$\gamma$
E	—	$\delta$
F	F	$\epsilon$
—	G	—
—	H	—
G	—	—
H	—	—
<hr/>		
I	a	a + b?
—	b	—
K	c	c
(duplication	c'	—
triplication)	c''	—
—	d	—
—	—	d
—	—	$F_6$
—	—	OSCP
—	—	—

$A_1/V_1/F_1$  subunits (below) are separated from the  $A_0/V_0/F_0$  subunits by a dashed line.

patterns and assembly strategies [3]. This review will summarize current knowledge of the structure and function of the ATP synthases/ATPases from the three domains of life, point out functional differences and discuss their possible structural basis. Finally, the evolution of structure and function of ATP synthases/ATPases will be discussed.

## Function and structure of $F_1F_0$ -ATPases

### The binding change mechanism of $F_1$ and the ATP synthase

Both  $F_1$  ATPase and ATP synthase display negative cooperativity in binding nucleotides, but positive cooperativity in catalysis. Boyer and colleagues [19] have shown that in the case of ATP synthase, the release of ATP (the product) is greatly enhanced by the binding of ADP +  $P_i$  to an adjacent catalytic site, located at the interfaces between the  $\alpha$  and  $\beta$  subunits [20], with the large majority of protein-to-nucleotide ligands provided by the  $\beta$  subunits. Similarly, the release of ADP +  $P_i$  is promoted by ATP binding to an adjacent catalytic site in  $F_1$  ATPase. To account for these observations, it has been proposed that the three catalytic sites alternate sequentially between the three different states, open, loose and tight, with different affinities for nucleotides. During ATP synthesis, energy from the ion translocation is used to convert a tight site into an open site, with the release of ATP. Simultaneously, the loose site, with bound ADP +  $P_i$ , is converted into a tight site, leading to ATP synthesis, while the open site, which has low affinity for nucleotides, is converted into a loose site ready to bind the substrates. During ATP hydrolysis in  $F_1$ , the reverse reaction operates. This model has been called the binding change mechanism [19]. The model assumes that one or two catalytic sites are occupied by ATP (or ADP) at any moment of steady-state catalysis [21] and has adapted the so-called bi-site catalysis. However, using the fluorescence of tryptophan introduced near the catalytic site as the signal of nucleotide binding, it has been shown that all three catalytic sites are occupied under physiological conditions. In the case of the *E. coli*  $F_1$ -ATPase MgATP binds in stoichiometric

amounts at the first catalytic site (single site) with high affinity ( $K_{d1} \approx 10^{-9}$  M; [22, 23]. Occupation of the second and third sites by MgATP occurs with significantly lower affinity (negative cooperativity;  $K_{d2} \approx 10^{-6}$  M,  $K_{d3} \approx 10^{-5}$  M). Furthermore, comparison of MgATP binding stoichiometry with hydrolysis data under steady-state MgATP hydrolysis showed that  $K_{d3}$  corresponds to the  $K_m$ -value, indicating that all three catalytic sites bind a nucleotide to attain the maximum hydrolysis rate (tri-site catalysis) [24].

### Structure of the $F_1$ domain

$F_1$  can be easily and reversibly dissociated from  $F_0$  as a soluble enzyme that only hydrolyzes ATP and is often called  $F_1$ -ATPase. Significant insights into the molecular mechanism of ATP hydrolysis came from the X-ray analysis of the  $\alpha_3\beta_3\gamma$  complex of the bovine  $F_1$ -ATPase [25]. The crystallographic model shows that the three  $\alpha$ 's and  $\beta$ 's are alternatively arranged in a hexameric ring forming a large central cavity in which half of the long coiled-coil  $\gamma$  subunit is inserted (fig. 2). This coiled-coil structure of subunit  $\gamma$  is asymmetrically located in the shaft relative to the axis of the  $\alpha_3\beta_3$  complex and protrudes from it by about 30 Å into the stalk region. A third short  $\alpha$  helix of the  $\gamma$  subunit is inclined at a 45° angle to the coiled-coil domain at the bottom of the  $F_1$  as it merges with the stalk that connects the  $F_1$  and  $F_0$  parts. A key feature of the structural model is its asymmetry, particularly in the nucleotide occupancy and conformations of the catalytic  $\beta$  subunits. One  $\beta$  subunit, designated  $\beta_{TP}$ , contains the ATP analogue MgAMP · PNP and is linked to the short  $\alpha$  helix of the  $\gamma$  subunit via the C-terminal domain. A second  $\beta$  subunit,  $\beta_{DP}$ , has MgADP bound, and

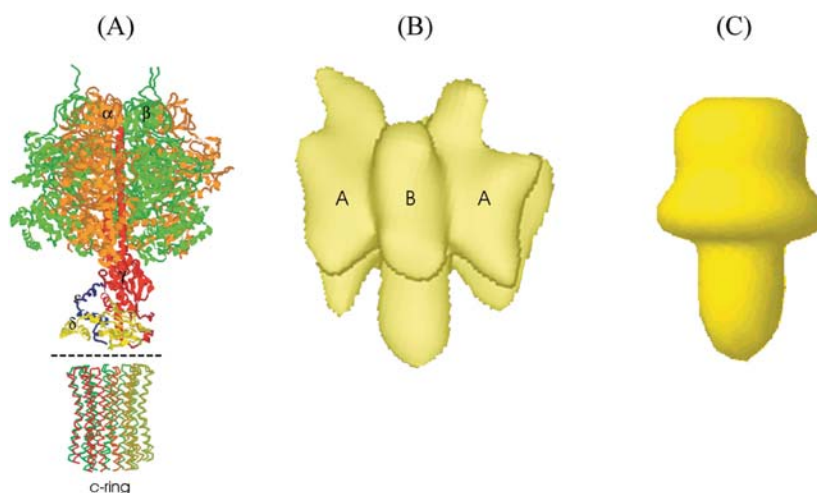


Figure 2. Comparison of the crystal structure of the  $F_1F_0$ -ATP synthase (A), the three-dimensional reconstruction of the  $V_1$ -ATPase without subunit C from *M. sexta* ((B), [85]) and the low-resolution envelope of the *M. mazei* Gö1  $A_1$ -ATPase (C) [87]. The  $F_1$ -complex was determined from the bovine [32] and the  $c$ -ring ( $c_{10}$ ) – presented below the dashed line – from the *S. cerevisiae* ATP synthase [35], respectively. The crystallographic coordinates were taken from the Brookhaven Protein Data Bank [174], entries 1E79 and 1QO1.

the third catalytic site,  $\beta_E$ , is empty. The three noncatalytic  $\alpha$  subunits are occupied with MgAMP · PNP and adopt similar conformations [25, 26]. A novel crystal structure of bovine  $F_1$  [27], with all three catalytic sites occupied by nucleotides, shows the complex in the presence of MgADP and aluminium fluoride ( $AlF_4$ ). Two  $\beta$  subunits bind MgADP- $AlF_4$  and were identified as being equivalent to  $\beta_{TP}$  and  $\beta_{DP}$  in the structure of the bovine  $\alpha_3\beta_3\gamma$  complex (see above) regarding their relative positions to the asymmetric  $\gamma$  subunit. Their structures are similar to each other, whereby the catalytic sites are not equivalent, due to the different relative positions of the corresponding  $\alpha$  subunits (which contribute residues to the catalytic sites). The third  $\beta$  subunit equivalent to  $\beta_E$  takes a half-closed conformation and retains MgADP and a sulfate at the catalytic site. This conformation is proposed to represent the posthydrolysis product state, with the sulfate group mimicking the cleaved  $\gamma$  phosphate. However, in this form, the C-terminal domain of  $\beta$  swings about 23° upwards, and the distance between the  $\beta$ -phosphate of ADP and the sulfate would be too long to resynthesize ATP, even if sulfate were replaced by phosphate. Notably, the molecular structures of the rat liver [28] and the chloroplast  $F_1$  [29] have been determined in the absence of magnesium and show that all  $\alpha$  and  $\beta$  subunits appear to have the closed conformation, implying that the asymmetry of the catalytic sites in  $F_1$  is controlled by magnesium and subunit  $\gamma$ . However, if the objective of future structural studies on  $F_1$  is to understand the mechanism of ATP synthesis/hydrolysis, it may be most profitable to obtain crystals containing all of the physiological substrates for ATP synthesis/hydrolysis.

### Structural features of the central stalk subunits

Until recently, the atomic structure of the protruding part of the central stalk of  $F_1$  was not resolved because of presumed disordering. Analysis of crystals containing the  $\alpha_3\beta_3\gamma\epsilon$  complex of *E. coli*  $F_1$  revealed that subunit  $\gamma$  extends from the  $\alpha_3\beta_3$  hexagon far enough to traverse the full length of the central stalk [30], in agreement with the refined crystal structure at 2.4 Å resolution of the  $\gamma$ - $\epsilon$  complex from *E. coli* [31] and the complete bovine  $F_1$ -ATPase, inhibited with dicyclohexylcarbodiimide (DCCD) (fig. 2; [32]). In these structural models the  $\gamma$  subunit is arranged in six  $\alpha$  helices and five  $\beta$ -stranded  $\beta$  sheets [31, 32]. The bottom of  $\gamma$  is in contact with the external loop of subunit  $c$  [33–35] (fig. 2). Adjacent to the 'bottom' part of subunit  $\gamma$  an additional density has been observed in both electron density maps [31, 32], and the structure of the  $\epsilon_{cc}$  subunit [36], the counterpart of the bovine  $\delta$  subunit (fig. 1;  $\delta_m$ ), has been modelled in these densities. Like subunit  $\epsilon_{cc}$ , the subunit  $\delta_m$  is composed of a C-terminal helix-loop-helix structure and an N-terminal 10-stranded  $\beta$ -sandwich structure. The modelling of the

$\epsilon_{cc}$  subunit indicates that the C-terminus of the polypeptide is turned away from the bottom domain of the catalytic  $\beta$  subunit. This domain is believed to be involved in the coupling of ATP hydrolysis/synthesis in the catalytic subunits along with  $\gamma$  and  $\epsilon_{cc}$  acting as a rotor (reviewed in [17]). The position of the C-terminal  $\alpha$ -helical domain of  $\epsilon$  differs from the model of the  $\gamma_{cc}$ - $\epsilon_{cc}$  subcomplex [31] and the reevaluated electron density map of the *E. coli*  $\alpha_3\beta_3\gamma\epsilon_{cc}$  complex [37], in which these two C-terminal  $\alpha$  helices are separated and stretch upwards to contact the  $\alpha_3\beta_3$  hexamer. Most recently, these two arrangements have been trapped in the *E. coli*  $F_1F_0$ -ATP synthase [38]. With the C-terminal domain of  $\epsilon$  towards  $F_0$ , as in the bovine structure, ATP hydrolysis is activated, but the enzyme is fully coupled in both ATP hydrolysis and synthesis. With the C-terminal  $\alpha$  helices toward the  $F_1$  domain, ATP hydrolysis is inhibited and yet the enzyme is fully functional in ATP synthesis. However, it is not yet possible to be precise about the distinct positions of the C-terminal domain of  $\epsilon$  during ATPase function.

The electron density map of the DCCD-inhibited form of the bovine  $F_1$ -ATPase also reveals the structure of the mitochondrial  $\epsilon$  subunit ( $\epsilon_m$ ), which has no counterpart in the bacterial  $F_1F_0$  and completes thereby the inside of the central stalk subunits (fig. 2). The 50 amino acid  $\epsilon_m$  has a helix-loop-helix structure and appears to stabilize the foot of the central stalk, where the  $\gamma$ ,  $\delta_m$  and  $\epsilon_m$  subunits all interact extensively [5, 25]. It is likely that all three subunits contact the  $F_0$  domain.

### Structure and function of the $F_0$ domain

The  $F_0$  domain in its simplest form as encountered in most bacteria consists of three subunits,  $a$ ,  $b$  and  $c$ , in a stoichiometry of 1:2:9–14 which mediate ion flow through the cytoplasmic membrane [1]. A high-resolution structure of the complete  $F_0$  is not available. Subunit  $b$  contains two transmembrane  $\alpha$  helices [39] and a rather large cytoplasmic domain which is proposed to be a part of the peripheral stalk [40, 41] (fig. 3). The crystal structure of the cytoplasmic domain of  $b$  (residues Thr<sub>62</sub>–Lys<sub>122</sub>) is characterized by a monomeric  $\alpha$  helix with a length of 90 Å [42]. Subunit  $b$  is not involved in ion transport across the cytoplasmic membrane which is catalyzed by the membrane-embedded subunits  $a$  and  $c$ . Extensive mutagenesis studies revealed that residues Arg-210, His-245 and Glu-219 of subunit  $a$  (*E. coli* numbering) are involved in ion transport [43–45], but recent studies revealed that only Arg-210 is essential for ion conduction [46]. This residue is in close proximity to the active carboxylate of subunit  $c$  (Asp-61 in *E. coli*) [44, 46, 47], and as we shall see later, both residues are key players in ion transport. The structure of subunit  $a$  is not known. Secondary structure analyses predict five or six transmembrane helices, and both models are supported

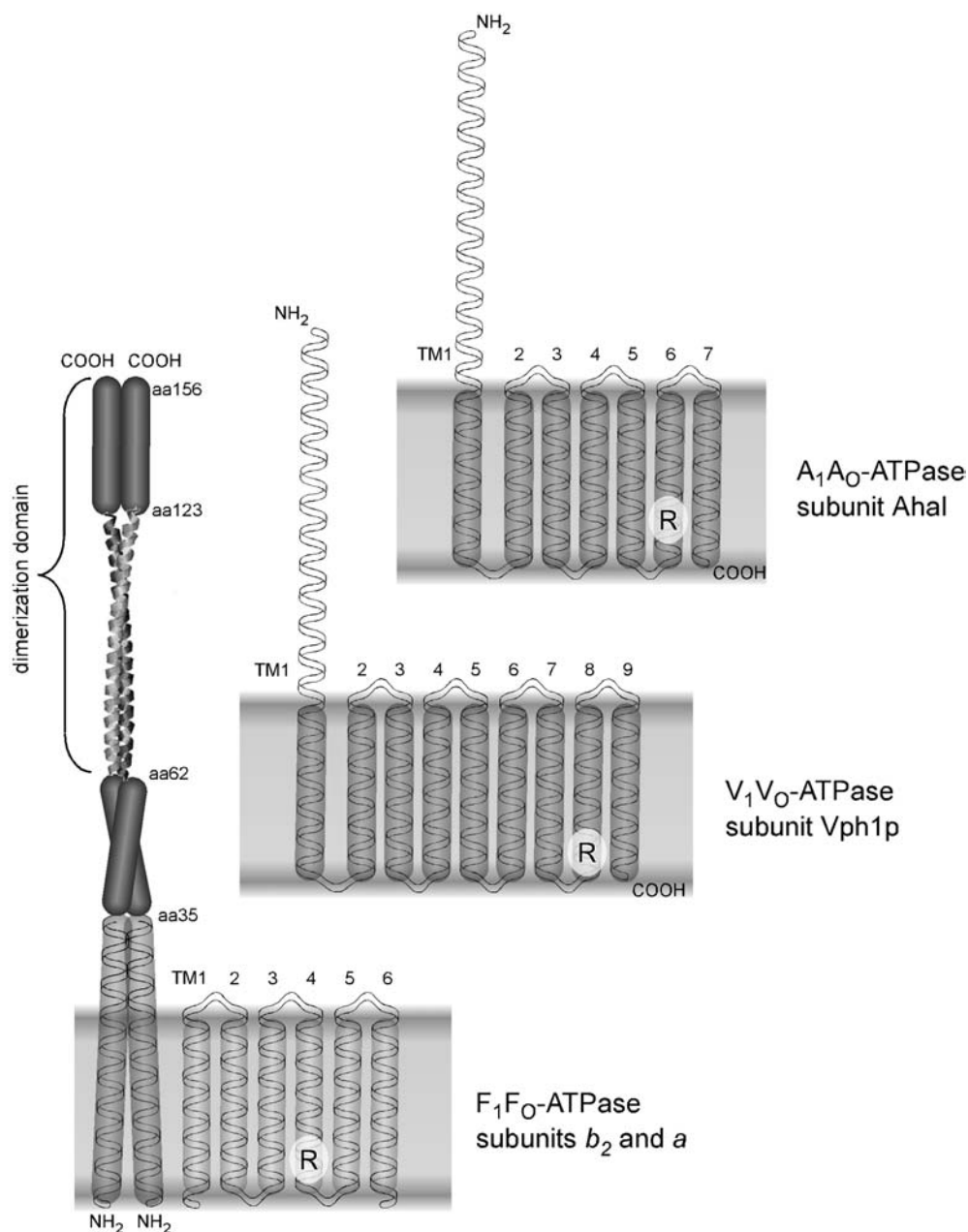


Figure 3. Proposed secondary structures and topology of subunits *a* and *b* of bacterial F-type ATPases, subunit *a* of V-type ATPases and subunit I of A-type ATPases. *R*, indicates the specific Arg-residue involved in ion translocation. The helical arrangement of the peptide encompassing residues Met1–Ile33 and the three-dimensional structure of the peptide Thr62–Arg122 of subunit *b* derived from nuclear magnetic resonance (NMR) [37] and crystallographic data [42], respectively. For explanations, see text.

by experimental evidence [48–50]. Furthermore, not only the number of transmembrane helices but also the cellular localization of the N and C termini are currently under debate [51–52].

Subunit *c* has two transmembrane  $\alpha$  helices that are connected by a cytoplasmic loop. The active carboxylate (aspartate or glutamate, Asp-61 in *E. coli*; fig. 4) which undergoes protonation/deprotonation cycles during H<sup>+</sup> transport is located in helix 2 [53]. Structural data show the *c* polypeptides arranged in a ring with a stoichiome-

try of 10, 11 and 14 *c*'s in yeast [35], *Ilyobacter tartaricus* [54, 55] and chloroplasts [56], respectively. Because biological function was not proven, it is not clear whether the different stoichiometries are the result of purification artifacts or indeed represent the in vivo structure. The structure of this ring is unknown, but it is assumed that the subunit *c* monomers are arranged in a front-to-back type giving two concentric rings. It is still a matter of debate whether helix 1 or 2 makes the outer ring of the oligomer [57–60]. One of the critical questions impor-



tant for the mechanism of ion translocation is the position of the active carboxylate relative to the cytoplasmic membrane. Two models were proposed, in which the active carboxylate resides either in the cytoplasmic membrane [58, 61] or at the cytoplasmic site [62, 63]. However, most recently, the cytoplasmic site model was revised [55, 64].

Subunit *c* contacts the central stalk of the enzyme by an interaction of the cytoplasmic loop with subunit  $\gamma$  and  $\epsilon$  [33, 34]. Electron microscopy [65] as well as atomic force microscopy [66] revealed that subunit *a* is located outside the ring of *c* subunits, and it is speculated that the ion passes through the interphase between subunits *a* and *c* [61].

The  $F_1F_0$ -ATPase operon from *Actobacterium woodii* differs from all other  $F_1F_0$ -ATPase operons known by the presence of three genes encoding proteolipids (fig. 4; [67]). AtpE<sub>2</sub> (subunit *c*<sub>2</sub>) and AtpE<sub>3</sub> (subunit *c*<sub>3</sub>) are 100% identical on the amino acid level, and only 18 substitutions occurred on the DNA level. This is strong evidence for duplication of an ancestral gene. The deduced molecular mass of the polypeptides is 8.18 kDa. AtpE<sub>1</sub> is more than double the size of AtpE<sub>2/3</sub>. The first and second halves are 66% identical on the DNA level, indicating a duplication of a precursor and subsequent fusion of the two gene copies. The deduced molecular mass of AtpE<sub>1</sub> (subunit *c*<sub>1</sub>) is 18.37 kDa, with four predicted transmembrane helices arranged in two hairpins, but the membrane-buried ion-binding residue (Glu-62 in AtpE<sub>2/3</sub>) is substituted by a glutamine residue in hair pin 2 (fig. 4). Western blot analyses revealed the presence of both 8- and 16-kDa proteolipids in the  $F_1F_0$ -ATPase from *A. woodii* [68]. The proteolipid oligomer of the  $F_1F_0$ -ATPase from *A. woodii* is the first known to contain a mixture of 8- and 16-kDa polypeptides [69]. The heterooligomeric structure could give rise to an alternative mechanism of ATPase regulation (see below). However, the stoichiometry of the different polypeptides in the *c* oligomer has not yet been determined.

Although most  $F_1F_0$ -ATPases use H<sup>+</sup> as coupling ion, the enzymes from the anaerobic bacteria *Propionigenium modestum*, *A. woodii* and *I. tartaricus* use Na<sup>+</sup> as the coupling ion under physiological conditions [69, 70]. Apparently, only a very few changes are required for changing the ion specificity of  $F_1F_0$ -ATPases. In addition to the active carboxylate in subunit *c*, an adjacent serine or threonine residue in the same helix and a glutamine in helix 1 were identified by mutagenesis studies to be involved in Na<sup>+</sup> liganding, and sequence comparisons led to the hypothesis that a fourth residue, a proline in helix 1 may be engaged in Na<sup>+</sup> binding [71–73] (fig. 5). Whether there is an additional specific Na<sup>+</sup>-binding motif in subunit *a* remains to be seen, but sequence analyses revealed a very strong similarity in the C terminus of subunit *a* of Na<sup>+</sup>- $F_1F_0$ -ATPases [74]. Clearly, the discussion on the function of the F<sub>0</sub> domain is hampered by the lack of high-resolution structures.

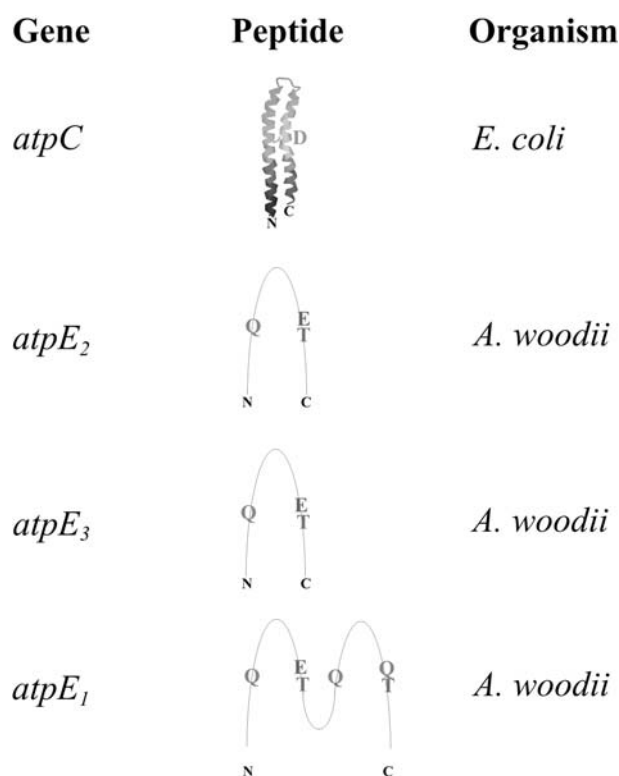


Figure 4. Gene-polypeptide correspondence of subunits *c* [175] and *c*<sub>1</sub>, *c*<sub>2</sub>, *c*<sub>3</sub> from the  $F_1F_0$ -ATP synthase of *E. coli* and *A. woodii*, respectively. The amino acids proposed to be involved in ion conduction are indicated. The potential Na<sup>+</sup>-binding proline residue is not indicated (cf. fig. 5). The NMR coordinates were taken from the Brookhaven Protein Data Bank [174], entry 1A91.

The F<sub>0</sub> domain is a rotational motor with subunits *a* and *b* being part of the stator and subunit *c* being the rotor. For further discussion of the function of the F<sub>0</sub> domain, see below.

## Structure and mechanism of V<sub>1</sub>V<sub>0</sub>-ATPases

### Structure of the V<sub>1</sub> domain

Whereas the F<sub>1</sub> and F<sub>0</sub> sectors described above form a stable associated complex in the cell, a fundamental difference to the V<sub>1</sub>V<sub>0</sub>-ATPases is the reversible dissociation of V<sub>1</sub> from the V<sub>0</sub> complex as an *in vivo* regulation, as shown during moulting [75] and response to glucose withdrawal [76] in the tobacco hornworm *Manduca sexta* and yeast, respectively. In both insects and yeast, disassembly of V<sub>1</sub> resulted in decrease of Mg-ATPase activity and proton pumping at the membrane, and reassembly restored these activities [77, 78]. Notably, neither disassembly nor reassembly requires new protein synthesis. The recovery of disassembled V<sub>1</sub> particles from the cytoplasm in high yield and purity [79] made the structural determinations possible.

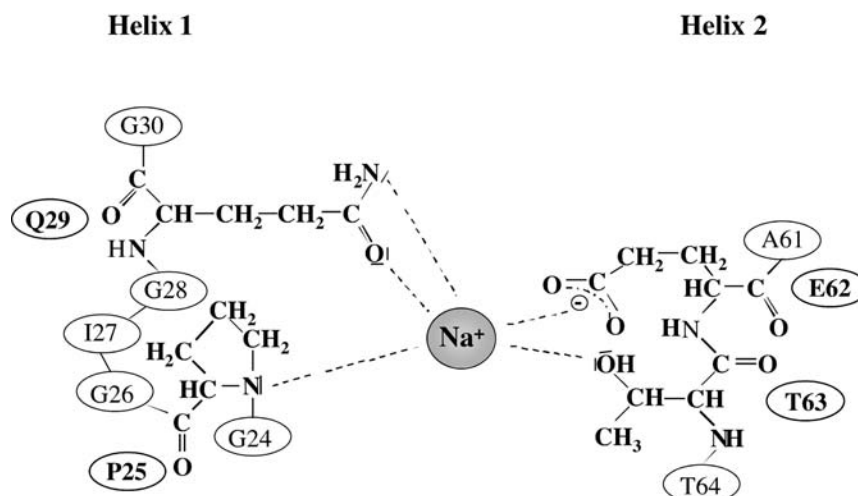


Figure 5. The proposed  $\text{Na}^+$ -binding motif in subunit *c* of  $\text{F}_1\text{F}_0$ -ATPases. Residues (proposed) to be involved in  $\text{Na}^+$  binding (Pro-25, Gln-29, Glu-62, Thr-63, *A. woodii* numbering) are given. The involvement of Pro-25 is based on sequence comparisons only. For explanations, see text.

The  $V_1$  domain has a mushroom-like shape [80] and comprises the catalytic subunit A and the nucleotide-binding subunit B in a stoichiometry of  $\text{A}_3\text{B}_3$ , and the so-called stalk subunits C–H in a proposed stoichiometry of  $\text{C}_1\text{D}_1\text{E}_1\text{F}_1\text{G}_2\text{H}_1$  [81]. A comparison of independently identified  $V_1$  structures [80, 82–84] reveals that the A and B subunits are hexagonally arranged, and alternate around a central cavity of approximately 3.2 nm in which a seventh mass is located [85]. A recent three-dimensional structure of the  $V_1$ -ATPase from *M. sexta* at 18 Å resolution (fig. 2) shows that the seventh mass is not located in the center of the cavity of the  $\text{A}_3\text{B}_3$  hexamer, but slightly offset to one side, leading to stronger connection of two nonneighboring A subunits [85]. This feature is comparable to the asymmetric location of subunit  $\gamma$  in the  $\alpha_3\beta_3$  subcomplex, linking two different occupied catalytic subunits,  $\beta_{\text{TP}}$  and  $\beta_{\text{E}}$  (see above; [25]). Seen from the side the structure shows three protuberances at the top of the  $\alpha_3\beta_3$  headpiece, which might belong to the N termini of subunit A [18, 84–86]. At the bottom side of the  $\alpha_3\beta_3$  domain the stalk protrudes with an angle of approximately  $7^\circ$  with the vertical axis of the cavity. The shape of the stalk resembles the stalk domain of the related  $\text{A}_1$ -ATPase of *Methanosarcina mazei* Gö1 [87] (fig. 2).

The only component of the  $V_1$ -ATPase solved at atomic resolution (3.0 Å) is subunit H [88], which has no homolog in A- or F-ATPases. This elongated subunit is required for V-ATPase function [89, 90] and interacts with the subunits B, E and F as shown by cross-linking experiments [84, 91]. Subunit H is characterized by the large, primarily  $\alpha$ -helical N-terminal domain, forming a shallow groove, and the C-terminal domain, both connected by a four-residue loop [88].

Differential protease sensitivity, release by chaotropic agents and cross-linking studies have been used to obtain

topological models of the stalk subunits inside the  $V_1$  complex [81, 84]. These studies have shown that the subunits C, E, G and H are exposed in the complex. Although the energy transduction mechanism of V-ATPase is predicted to be similar to that of F-ATPases, it is still under discussion whether subunit D [92, 93] or E [84, 94, 95], both highly  $\alpha$  helical, correspond to the  $\gamma$  subunit of F-ATPases. Xie [96] reported that at least the A, B, C, E and G subunits, but not the D and F subunits, are essential for ATP hydrolysis in the bovine enzyme. This is in line with most recent experiments in which a stable  $\text{A}_3\text{B}_3\text{CE}$  and  $\text{A}_3\text{B}_3\text{EG}$  subcomplex with high ATPase activity have been observed from the clathrin-coated vesicle  $\text{H}^+$ -ATPase [97] and from *M. sexta* V-ATPase [V. F. Rizzo, Ü. Coskun and G. Grüber, unpublished data], respectively. Recently determined low resolution structures of the  $V_1$ -ATPase from *Caloramator fervidus* [82] and *M. sexta* [80, 85] revealed a molecule with a single, compact stalk, but no peripheral stalk. Side-view projections of negatively stained  $V_1V_0$ -ATPases from *C. fervidus* show a peripheral stalk, proposed to be formed by the  $V_0$  portion and to function as a stator [14]. More recently, a second peripheral stalk in the  $V_1V_0$ -ATPase has been described from negatively stained images [15, 86, 98]. These structural data pose the question, which subunits comprise the putative second stator, and does the  $V_1$  complex become more compact following dissociation, with the peripheral stalk collapsing into a single stalk in free  $V_1$ -ATPase?

### Structure of the $V_0$ domain

The  $V_0$  domain is comprised of at least five subunits, *a*, *d*, *c*, *c'*, and *c''*. Subunit *a* is a two-domain protein and combines functional and structural features of subunits *a* and *b* of F-ATPases [99] (fig. 3). The large, N-terminal hydrophilic domain interacts with both subunits H and A

[100], and therefore it is most likely part of the second stalk (the stator). Interestingly, there is only one copy of subunit *a* in  $V_O$ , whereas there are two copies of subunit *b* in  $F_O$ . The role of the missing 'soluble *b*' could be taken over by subunit *G*, which has some sequence similarity to the 'soluble *b*' of F-ATPases [101]. The C-terminal domain of subunit *a* is very hydrophobic and predicted to span the membrane nine times. Mutagenesis studies have identified several membrane-buried residues important for function, but as with subunit *a* of F-type ATPases, only one Arg residue (Arg-735 of *Saccharomyces cerevisiae*) was shown to be essential for ion transport [99]; this residue is most likely the essential positive charge on the stator (see below). Recently, Arg-573 of subunit *a* of *Enterococcus hirae* was identified to be involved in  $Na^+$  binding [102].

Subunits *c*, *c'* and *c''* are similar to each other and to other proteolipids from F-, A- and V-type ATPases. Subunits *c* and *c'* are twice the size of the 8-kDa proteolipids from bacteria and most archaea, and arose by duplication and fusion of an ancestral proteolipid gene giving rise to a 16-kDa protein with four transmembrane helices [103, 104]. Importantly, the active carboxylate was conserved in TM4, but not in TM2. Subunit *c''* is even bigger and has five predicted transmembrane helices, with the active carboxylate conserved only in TM3. Elegant studies clearly demonstrated that each  $V_O$  domain contains at least one copy of *c*, *c'* and *c''* [104], and it is assumed that the number of transmembrane helices in F-, V- or A-ATPases is similar (~24 transmembrane helices, see above). Therefore, the number of proton translocating residues in  $V_O$  is only half of that in  $F_O$ .

Subunit *d* is a completely hydrophilic, cytoplasmic protein but copurifies with the  $V_O$  complex and, therefore, it is regarded as a  $V_O$  subunit [105]. Its function is unknown, but it could be involved in regulation of ion conductance through  $V_O$ .

Recently, a sixth subunit (*e*) of the  $V_O$  domain was described for the V-ATPase of the *M. sexta* midgut [106], bovine chromaffin granules [107] and *Arabidopsis thaliana* [108], with apparent molecular masses of 9.7, 9.2 and 7.8 kDa, respectively. Until now, nothing is known concerning its function. Interestingly, the homolog to these polypeptides in yeast is Vma21, resident in the endoplasmic reticulum and there involved in assembly processes of the V-ATPase [109].

The coupling ion in most of the V-ATPases studied to date is the proton. However, two anaerobic bacteria, *Caloramator fervidus* [110] and *E. hirae* [111], contain  $Na^+$ -translocating ATPases of the A/V type (for classification, see below). Both are fermenting anaerobes that have a rather low energy yield obtained only through substrate level phosphorylation. *C. fervidus* is a thermophile, and *E. hirae* produces the  $Na^+$ -translocating A[V]-ATPase only at alkaline conditions. In both cases,  $Na^+$ -based

membrane energization is energetically advantageous over the use of protons [112, 113]. The proteolipid of the A[V]-ATPases from *E. hirae* contains the sodium ion binding motif, and the active carboxylate has been identified experimentally to be involved in  $Na^+$  binding [114]. Nothing is known about  $Na^+$  binding in subunit *a*.

## Properties and function of the archaeal A-ATPase

### Structure and function of the $A_1$ domain

The  $A_1$  complex of archaeal ATPases possesses a pseudo-hexagonal arrangement of six peripheral globular masses, reflecting the major subunits A and B, as proposed from two-dimensional images of the thermoacidophilic archaea *Sulfolobus acidocaldarius* and *Methanosarcina mazei* Gö1 [115, 116] (see figs 1, 2). Photoaffinity labelling with the nucleotide analog 2- $N_3$ -ATP showed that both subunits can be labelled with a preference for subunit A [117]. This is in agreement with the fact that subunit A contains the Walker motifs A and B [118], which are critical for nucleotide binding [25], and that the conserved motif G-X-X-X-G-K-T is present in subunit B 195 amino acids downstream of the expected nucleotide binding site [3]. In contrast to the related  $F_1$ -ATPases described above, little is known about the overall structure and the subunit topology of this complex. Two major advances towards an elucidation of the quaternary structure of the  $A_1$ -ATPase have been made during the last years. First, a fragment containing *ahaE*, *ahaC*, *ahaF*, *ahaB*, *ahaA* and *ahaG* of the  $A_1A_O$ -ATPase operon from the methanogenic archaeon *M. mazei* Gö1 was cloned in an overexpression vector and transformed into the  $F_1F_O$ -ATPase negative mutant *E. coli* DK8 which produced an  $A_1$ -ATPase upon induction of gene expression [119]. Second, an  $A_1A_O$ -ATPase containing 9 of the 10 subunits deduced from the DNA sequence could be purified from the hyperthermophilic methanogenic archaeon *Methanococcus jannaschii* [A. Lingl and V. Müller, unpublished data].

The  $A_1$  complex heterologously produced in *E. coli* is made up of the five different subunits A–D and F with molecular masses of 64, 51, 41, 24 and 11 kDa, as estimated from the amino acid sequences [116]. Their localization within the complex is not clear (but see below), but homologs could be identified in other ATPases (see table 1). A model-independent approach, which is based upon the multipole expansion method using spherical harmonics [120], has been used to study the three-dimensional envelope of the  $A_3B_3CDF$  complex from solution X-ray scattering (fig. 2; [80]). The determined complex is asymmetric, with a headpiece which is ~94 Å long and 92 Å wide, and a stalk with a length of ~84 Å and 60 Å in diameter that accounts for linking catalytic site events in the  $A_1$  headpiece with ion pumping through the  $A_O$  do-



main [87]. Superposition of the low-resolution structure of the  $A_1$  complex with the atomic model of the  $\alpha_3\beta_3\gamma$  complex of the related  $F_1$ -ATPase from *E. coli* [30] reveals a striking similarity, especially with respect to the disposition of the nucleotide-binding subunits  $\alpha$  and  $\beta$ , the homologs of subunits B and A, respectively [87]. This structural similarity lends support to the view that A- and F-ATPases share a common catalytic mechanism for ATP synthesis.

Further insights into the topology of the  $A_1$ -ATPase were obtained by tryptic digestion. These studies have shown that the subunits C and F are exposed in the complex, whereas subunit D is well protected from the effect of trypsin [87]. The shielding of subunit D from trypsin is an important finding since this subunit has been proposed as the structural and functional homolog of the  $\gamma$  subunit of F-ATPases [3, 11]. Most recently, it has been shown that subunit D can be cross-linked to the catalytic A subunit depending on nucleotide binding. An A-D-A formation occurs after addition of MgADP and to a small extent in the presence of the hydrolyzable MgATP but not in the presence of MgADP+Pi, MgAMP-PNP or the absence of nucleotides. This interaction between A and D involves the N and C termini of subunit D [121], whose secondary structures are predicted to be  $\alpha$  helical [116], as described for both termini of subunit  $\gamma$  of  $F_1$  [25]. The X-ray structure of  $F_1$  reveals that the  $\alpha$ -helical N and C termini of  $\gamma$  intercalate into the cavity of the  $\alpha_3\beta_3$  assembly of  $F_1$ , thereby linking two differently occupied catalytic subunits,  $\beta_{TP}$  and  $\beta_{DP}$  [25]. Therefore, binding of D to the catalytic A subunit of  $A_1$  followed by release may play a part in coupling the catalytic sites with the stalk region.

In general, significant structural alterations occur in the  $A_1$ -ATPase due to nucleotide binding. Small-angle X-ray studies showed that the value of the radius of gyration,  $R_g$ , increases slightly when MgATP, MgADP or MgADP+Pi are present, whereby binding of the unhydrolyzable MgAMP-PNP causes a slight decrease [121]. Such conformational changes of the quaternary structure are consistent with alterations in the related  $F_1$ -ATPase, as demonstrated in the most recent crystallographic model of bovine  $F_1$ -ATPase [27], in which significant changes of the lower part of the nucleotide binding domain and the C-terminal domain of the catalytic  $\beta$  subunits have been observed depending on nucleotide binding. The conformational changes in the  $A_1$  headpiece due to nucleotide occupation correlate with structural alterations in the stalk region, which can be expected when the stalk couples ATP hydrolysis/synthesis with ion conduction. Subunit C and F, shown to be exposed  $A_1$  stalk subunits, are less accessible to trypsin in the presence of MgATP as in the presence of MgAMP-PNP [121].

It is interesting to note that subunits E and G were not present in the purified complex. The homolog of subunit E is not obvious from sequence comparisons, but it was sug-

gested that subunit E might be homologous to subunit  $\delta$  of  $F_1F_0$  ATPases [3]. However, subunit E is required neither for assembly nor for function. Genome sequencing revealed *ahaG* homologs at the same position in the *atp* operons from *M. mazei* Gö1 [122], *Methanosarcina acetivorans* [123] and *Methanosarcina barkeri* [124] but not in other archaea. So far, production of subunit G could not be demonstrated in *M. mazei* Gö1 [T. Lemker and V. Müller, unpublished]. Therefore, it is still unclear whether *atpG* is an authentic ATPase gene.

### Structure and function of the $A_0$ domain

The  $A_0$  domain contains only two membrane-intrinsic subunits, I and K. The molecular mass of subunit I ranges from 72 to 76 kDa [3]; it is very similar to subunit *a* of  $V_1V_0$ -ATPases with a hydrophilic N terminal and a hydrophobic C-terminal domain of apparent molecular masses of  $\sim 39$  and  $\sim 33$  kDa, respectively, in *M. mazei* Gö1 (fig. 3). The hydrophilic domain is predicted to be highly  $\alpha$  helical and assumed to be the functional homolog of the soluble domain of subunit *b* of  $F_1F_0$ -ATPases. As discussed above for subunit *a* of V-type ATPases, the missing 'soluble *b*' homolog could be provided by subunit H. In this context is interesting to note that the gene encoding subunit H precedes the gene encoding subunit I. The hydrophobic C terminus of subunit I is predicted to have seven transmembrane helices and is assumed to be functionally similar to subunit *a* of  $F_1F_0$ -ATPases; however, similarity on amino acid sequence level is below 20%. The hydrophobic domain of Vph1p as well as subunit *a* of  $F_1F_0$ -ATPases are known to be involved in  $H^+$  translocation [125–128]. A multiple alignment of subunit I from A-ATPases and subunit *a* from V-ATPases reveals a high degree of conservation. The arginine essential for ion translocation (*a*Arg-735 in *Saccharomyces cerevisiae* [99]) is conserved in subunit I (equivalent to Arg-557 of *M. mazei* Gö1); this residue is most likely the essential positive charge on the stator in  $A_0$  (see below).

The homolog of subunit *d* of V-ATPases is not obvious, but it had been speculated, based on weak sequence similarity, that subunit C is similar to subunit *d* of V-ATPases [129]. Subunit K is synonymous with the proteolipid. Proteolipids have been purified and characterized from some archaea and in almost all cases they were shown to be of  $M_r \approx 8000$  with two transmembrane helices [116, 130–133]. Furthermore, with the exceptions mentioned below genome sequences predict 8-kDa proteolipids in archaea. This size corresponds to the size of the proteolipid from  $F_1F_0$ -ATPases and was hitherto assumed to be the reason for the  $F_1$ -like properties of the  $A_1A_0$ -ATPases, i.e. their function as ATP synthases. However, *M. thermoautotrophicus* and *M. jannaschii* have proteolipids with four and six membrane-spanning helices, respec-

tively. Apparently, the proteolipids from *M. thermoautotrophicus* and *M. jannaschii* arose by gene duplication and triplication, respectively, with subsequent fusion of the genes [134, 135]. In case of *M. thermoautotrophicus*, the ion-translocating carboxylate is conserved in helix 2 and 4, but in *M. jannaschii* it is only conserved in helix 4 and 6, in helix 2 it is substituted by a glutamine residue (fig. 6). The proteolipid from *M. jannaschii* is the first triplicated proteolipid found in nature and of particular importance for the concepts of ion translocation and its coupling to ATP synthesis.

So far, the ion specificity of  $A_1A_O$ -ATPases has not been addressed experimentally to a great extent. It was shown for only a few archaea that artificial  $H^+$  gradients drive the synthesis of ATP, but so far the use of  $Na^+$  as coupling ion was not demonstrated unequivocally (reviewed in [3]). The strictly anaerobic methanogenic archaea are unique among organisms because they couple the pathway of energy conservation with the primary extrusion of both  $Na^+$  and  $H^+$ . Claims have been made for  $H^+$ - as well as  $Na^+$ -driven ATP synthesis in *M. mazei* Gö1 and *M. thermoautotrophicus*, and inhibitor studies suggested the presence

of  $H^+$ -coupled  $A_1A_O$ - and  $Na^+$ -coupled  $F_1F_O$ -ATPases [136–139]. In contrast, genome studies clearly excluded the presence of  $F_1F_O$ -ATPase genes in *M. mazei* Gö1 [122] and *M. thermoautotrophicus* [140], but revealed the  $A_1A_O$ -ATPase genes. Therefore, the question how the  $Na^+$  gradient is converted to ATP synthesis is still open. Nevertheless, two related species, *Methanosarcina barkeri* and *Methanosarcina acetivorans* indeed have both  $A_1A_O$ - and  $F_1F_O$ -ATPase clusters in their genomes [123, 124]. However, an expression of the  $F_1F_O$ -ATPase genes of *M. barkeri* or the production of a functional  $F_1F_O$ -ATPase could not be demonstrated [T. Lemker and V. Müller, unpublished]. Future studies using the genetically tractable *M. acetivorans* should shed light on the enigma of the  $F_1F_O$ -ATPase genes in some methanogens.

Interestingly, inspection of the DNA sequence revealed the presence of the  $Na^+$  binding motif of subunit *c* of  $F_1F_O$ -ATPases in every methanoarchaeal proteolipid sequenced to date, but not in other archaea such as *Pyrococcus abyssi*, *Halobacterium salinarum* or *Sulfolobus acidocaldarius* [C. Weidner and V. Müller, unpublished]. This finding supports the hypothesis that the methanoar-

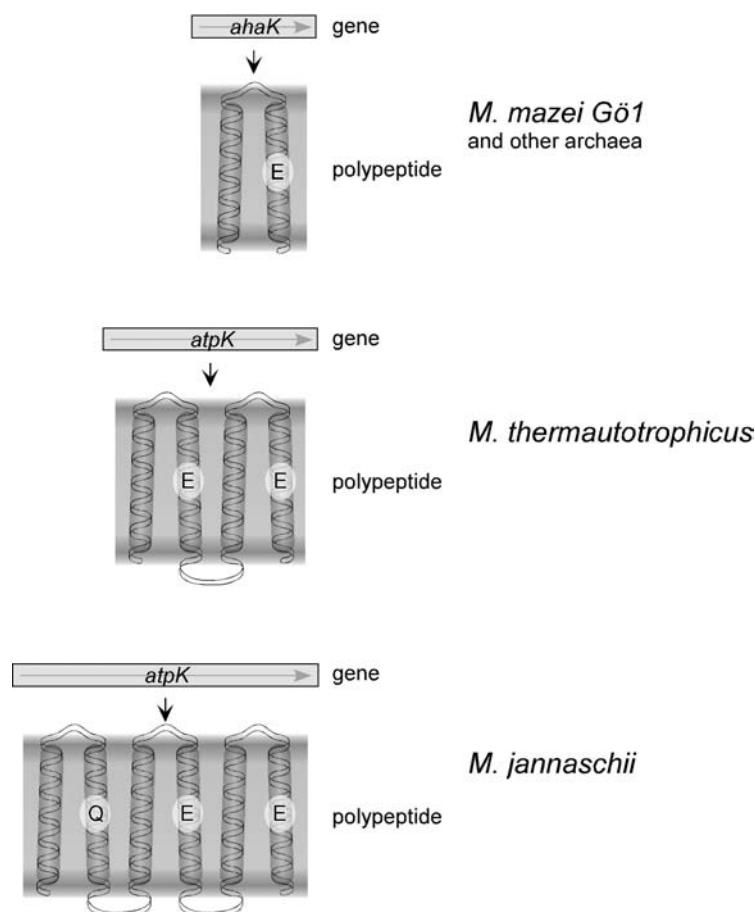


Figure 6. Gene-polypeptide correspondence of proteolipids from archaea. The duplicated and triplicated proteolipids of *M. thermoautotrophicus* and *M. jannaschii* arose by gene duplication and triplication events, respectively, followed by a fusion of the gene copies. The ion-translocating residues are indicated. For further explanations, see text.

chaeal  $A_1A_0$ -ATPase could also use  $\text{Na}^+$  as coupling ion. This question could not be addressed experimentally due to the fact that only subcomplexes of  $A_1A_0$ -ATPases were purified to date; none of the preparations contained subunit I, which is essential for ion translocation. However, the recently established protocol for the purification of a complete  $A_1A_0$ -ATPase from the hyperthermophile *M. jannaschii* [A. Lingl and V. Müller, unpublished] will enable an experimental approach addressing this question.

### The ATPases are rotatory machines

As discussed above, Boyer postulated already some time ago [19], based on kinetics of ATP hydrolysis, that the three  $\beta$  subunits of the F-ATPase are in a different state at any given time with respect to nucleotide occupation. But how are the conformational changes propagated between the sites, and how is this coupled to ion flow through the distantly located membrane domain? The key to this enigma came from the study of Walker, Leslie and co-workers who solved the structure of the bovine  $F_1F_0$ -ATPase at 2.8 Å resolution [25]. It showed the three  $\alpha\beta$  pairs in different conformations: one open, one closed having ATP bound and one partly open having ADP +  $\text{P}_i$  bound. Moreover, the structure also revealed an intrinsic asymmetry of the enzyme with the  $\gamma$  subunit in contact with only one  $\alpha\beta$  pair; this was suggested before from cryo-electronmicroscopy studies by Capaldi and co-workers (reviewed in [141, 142]). Furthermore, the structure revealed that subunit  $\gamma$  is protruding into the  $\alpha\beta$  hexagon as a shaft through a hydrophobic sleeve. All these observations strengthened the old hypothesis about rotation of subunits in  $F_1$  and led to a series of different experiments attempting to prove the concept of rotation. First, Cross and co-workers presented cross-linking experiments in which they first bound  $\gamma$  to a given  $\alpha\beta$  pair, then released the cross-link, formed a new one and found  $\gamma$  attached to a different  $\alpha\beta$  pair again [143]. The next step was done by Junge and co-workers, who introduced a fluorescence label onto subunit  $\gamma$  and demonstrated ATP-driven rotation of  $\gamma$  by polarized absorption recovery after photobleaching [144]. A direct visualization was achieved by Yoshida, Kinosita and co-workers who introduced a labelled actin filament onto subunit  $\gamma$  and demonstrated ATP-driven rotation of  $\gamma$  by an optical microscope [145]. In these experiments, a rotation by  $360^\circ$  in three  $120^\circ$  steps was observed. Recently, the same group observed rotational substeps of  $90^\circ$  and  $30^\circ$  by submillisecond kinetic analysis of the  $F_1$  complex [146]. These experiments gave unequivocal evidence for a rotation of subunit  $\gamma$  relative to the  $\alpha_3\beta_3$  hexagon during ATP hydrolysis.

However, the critical question still is how ion flow through  $F_0$  is driving rotation of subunit  $\gamma$  in  $F_1$ . Of course, a rotation of the  $c$  ring against subunit  $a$  which then drives rota-

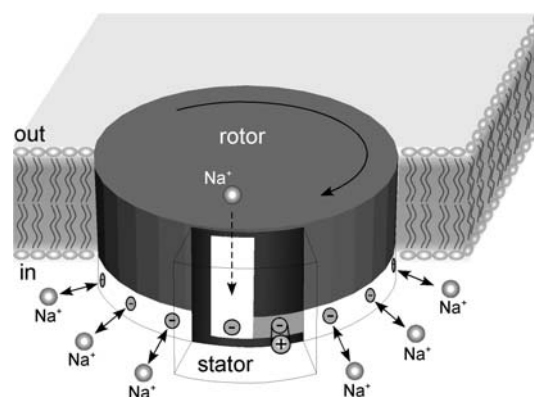


Figure 7. The motor of  $\text{Na}^+$ - $F_1F_0$ -ATPases. The rotor is made from proteolipid oligomers, and the stator function is provided by subunit  $a$ . The sodium ion binding site on the rotor is Gln-29, Glu-62, Thr-63 and probably Pro-25 (*A. woodii* numbering), and indicated by light green. The positive charge on subunit  $a$  is the well-conserved arginine (Arg-210 in *E. coli*). Adapted from ref. 62. For further explanations, see text.

tion of subunit  $\gamma$  would be the obvious answer. However, the final experimental evidence for a rotation of the  $c$  ring is still missing. The observation that subunits  $\gamma$ ,  $\epsilon$  and  $c$  as well as  $c$  subunits to each other can be cross-linked without loss of activity supported the idea of ion gradient-driven rotation of the  $c$  ring that then drives rotation of  $\epsilon$  and  $\gamma$  during catalysis, and additional cross-linking experiments demonstrated subunits  $a$ ,  $b$ ,  $\delta$ ,  $\alpha$  and  $\beta$  as part of the stator (reviewed in [52, 147]). In analogy to the experiments performed by Yoshida and co-workers with subunit  $\gamma$  [145, 146], several groups positioned a fluorescently labelled actin filament onto subunit  $c$  and could indeed demonstrate ATP-driven rotation of the  $c$  ring [148, 149]. Most recently, the observation of intersubunit rotation in fully coupled molecules of the  $\text{Na}^+$ -translocating ATP synthase of *Propionigenium modestum* during ATP synthesis or hydrolysis has been described [150]. Moreover, upon the incubation with the  $F_0$ -specific inhibitor DCCD the rotation was severely inhibited.

How does the motor function, i.e. convert electrochemical energy into torque generation? A major advance of our understanding of rotor function comes from experiments done with the  $\text{Na}^+$ - $F_1F_0$ -ATPase from *P. modestum* [151, 152] which will be summarized in the following and are illustrated in figure 7. The rotor component ( $c$  ring) is embedded into the cytoplasmic membrane and contains the ion binding site. The ion binding sites are freely accessible from the cytoplasm, but access from the periplasm is restricted and only possible by a not-well-defined channel, which leads to a negative charge on the rotor. In the close vicinity of the negative charge of the rotor subunits is the highly conserved positive charge of the stator (Arg-210) of subunit  $a$ . This residue is close to the ion channel and connected to it by a hydrophilic sleeve. Arg-210 of subunit  $a$  and a negative charge of the rotor

form a salt bridge, thereby fixing the rotor to that position. To the left of the hydrophilic stretch is a hydrophobic zone which prevents rotation of the *c* ring with non-occupied ion binding sites to the left. In the absence of a membrane potential, the rotor idles against the stator with no preference for direction of rotation; under these conditions, exchange of  $^{22}\text{Na}_{\text{in}}^+ / ^{22}\text{Na}_{\text{out}}^+$  occurs. Upon generation of a membrane potential, the rotor is forced to rotate into one direction. The membrane potential, therefore, is an essential component for ATP synthesis, and cannot be substituted by a chemical ion gradient. The ion enters the channel at its periplasmic entrance and traps a negative charge of the *c* monomer. This allows the ion to enter the hydrophobic zone and prevents it from going backwards. Thereby, the *c* oligomer rotates to the left. The rotor will now donate the ion to the cytoplasm due to the lower chemical activity of the ion inside. Charge regeneration on the rotor also prevents the rotor from going backwards. In the reverse reaction, ATP hydrolysis drives ion extrusion by the same mechanism. This model is supported by several lines of experiments and discussed in detail by Dimroth and co-workers [62]. However, it should be mentioned in this connection that a second model is discussed which assumes two half channels giving access of the rotor to the cytoplasmic and periplasmic side, respectively [61].

The sodium ion binding site of the ATPases of *A. woodii*, *P. modestum* and *I. tartaricus* has been identified by genetic and biochemical means to be Gln-32, Glu-65 and Ser-66 (*P. modestum* numbering); the serine residue is changed to a threonine residue in *A. woodii*. In addition, a fourth residue (Pro-28, *P. modestum* numbering) might be involved [73] (fig. 5). However, so far, a specific sodium ion binding site was not detected in subunit *a*. A triple mutation (K220R, V264E, I278N) of *P. modestum* subunit *a* was unable to translocate  $\text{Na}^+$  [153]; however, with the exception of Ile-278 these residues are not conserved in *A. woodii* and therefore it can be excluded that they are constituents of a specific sodium ion binding site [74]. Rather, the triple mutation most likely led to a perturbed overall structure of the channel not allowing entrance of  $\text{Na}^+$ .

Assuming a number of 12 negative charges per *c* oligomer and three ATP-binding sites in  $\text{F}_1$ , a stoichiometry of 4 protons (or a quarter of a full rotation) per ATP synthesized must be postulated. How can this stoichiometry be achieved mechanistically in a stepping motor? An experimentally supported model presented by Junge and co-workers suggests that subunit  $\gamma$  functions as an elastic power transmission shaft between the two motors  $\text{F}_0$  and  $\text{F}_1$  [154]. Such a mechanism could also readily explain the different  $\text{H}^+/\text{ATP}$  ratios observed with different enzymes that ranges from 3 to 4. It should be mentioned in this connection that alkaliphilic microorganisms are faced with the problem of a proton motive force of only  $-40$  to

$-60$  mV.  $\text{Na}^+$ -driven ATP synthesis was never observed, and therefore ATP synthesis can only be brought about by a  $\text{H}^+-\text{F}_1\text{F}_0$ -ATP synthase with a  $\text{H}^+/\text{ATP}$  stoichiometry of  $>10$  [113]. This could be achieved by a stiffer power transmission, but subunit  $\gamma$  from alkaliphiles is not obviously different, as based on primary sequence data. Therefore, the question how ATP is synthesized in alkaliphiles is still an enigma.

The overall similarities between F-, V- and A-ATPases might also reflect a mechanistic similarity in their operation. The rotor component of the A-type ATPase comprises at least the *c* oligomer and subunit D, the homolog of subunit  $\gamma$  the stator certainly contains subunit I and the  $\text{A}_3\text{B}_3$  hexagon. The localization of the other subunits is unknown, and the amino acid similarities to the minor subunits of F-ATPase are too low to identify the homologs [3]. The rotor component of the V-type ATPase also comprises at least of the *c* oligomer and subunit D or E, the proposed homolog of subunit  $\gamma$  the stator also certainly contains subunit *a* and the  $\text{A}_3\text{B}_3$  hexagon. However, the localization of the other subunits is also unknown [10]. Interestingly, it seems to emerge that V-ATPases might contain a second peripheral stalk that was visible in electron micrographs of the V-ATPase from *C. fervidus* [14]. More recently, a second peripheral stalk in the  $\text{V}_1\text{V}_0$ -ATPase has been described from negatively stained images [15, 86, 98]. Whether a second peripheral stalk is also present in A-ATPases remains to be identified. However, this is a challenging task for future structural work. The residues essential for motor function, i.e. the negative charge on the rotor component, and the positive charge on the stator component, are conserved in V- and A-ATPases (see above).

### Functional and structural differences of A-, F- and V-type ATPases

The discussion presented so far pointed out the similarities in the overall structure of the A-, F- and V-type ATPases. The best-understood specimen is the F-type ATPase, in which the function of the eight bacterial subunits is, in principle, understood [155]. This can be regarded as the minimal core unit of an ATP synthase. Of course, evolution fine-tuned the function of the enzyme, which required additional components. Furthermore, the evolution of structural cellular compartments added a new layer of complexity, which asked for additional components, e.g. proteins involved in transport, assembly, targeting and stabilization. Therefore, more gene products are required for function and assembly of the mitochondrial F-ATPase or the eukaryal V-ATPases. The 'core unit' of A- and V-type ATPases has evolved one additional subunit not found in F-ATPase, subunit C. The function of this subunit is not known, but it is located at the periphery of the central stalk of A- and V-ATPases [84, 87].



However, the evolution of the three classes of enzymes resulted in functional differences whose structural basis is not always obvious at this time.

A fundamental distinction of the three types of ATPases is the capability of isolated cytoplasmic domains to hydrolyze ATP. The reversible dissociation of the  $V_1$  from the  $V_o$  complex is an in vivo regulatory mechanism for the control of V-ATPase activity leading to  $V_1$  complexes of reduced MgATPase activity [75, 76]. Such a mechanism of control is not found in  $F_1F_o$ - and  $A_1A_o$ -ATPases and not required by the physiology of the cell or organelle employing  $F_1F_o$ - and  $A_1A_o$ -ATPases for ATP synthesis. The structural basis for this difference is unknown, but it is tempting to speculate that subunits exclusively found in V-type ATPases confer this special property to them.

As pointed out above, the most important functional difference of the A-, F- and V-type ATPases is their capability to synthesize ATP.  $F_1F_o$ - and  $A_1A_o$ -ATPases are engaged as ATP synthases under most cellular conditions and synthesize the enormous amount of ATP required for biomass production. However, the reaction  $ADP + P_i \rightleftharpoons ATP$  is completely reversible in vivo and in vitro, the direction of the reaction, net ATP synthesis or ATP-driven ion pumping, is only controlled thermodynamically or, in some special cases, by modification of the enzyme; the latter is known as thiol modification and is used in plants to inhibit ATP hydrolysis and to prevent loss of ATP in the dark [156]. This property of the F- and A-ATPases might be a result of their structure. The capability to synthesize ATP is directly dependent on the number of ions translocated per ATP synthesized. According to  $\Delta G_p = -n \cdot F \cdot \Delta p$ , a phosphorylation potential ( $\Delta G_p$ ) of  $\sim 50$  to  $70$  kJ/mol is sustained by the use of  $n = 3$ – $4$  ions/ATP at a physiological electrochemical ion potential of  $-180$  mV ( $\Delta p$ ). Because most F- and A-ATPases have 12 ion-translocating groups per enzyme or three  $\alpha\beta/AB$  pairs, this gives exact the number of ions required thermodynamically for ATP synthesis. As outlined above,  $V_1V_o$ -ATPases have a duplicated proteolipid with four transmembrane helices in which the ion-translocating group is only conserved in helix 4. Assuming a constant number of 24 helices in the  $c$  oligomer of ATPases, this would accommodate six copies of the monomer, but only six ion-translocating groups per proteolipid oligomer, half the amount as in F- and A-type ATPases. This results in a stoichiometry of only two ions per ATP which is too low to allow ATP synthesis at a  $\Delta G_p$  of  $\sim 50$  to  $70$  kJ/mol and a  $\Delta p$  of  $-180$  mV. However, the reduced  $H^+$ /ATP stoichiometry makes the enzyme a better proton pump, because the same  $\Delta G_p$  can account for a much higher  $\Delta p$ . Acidification of organelles is indeed the function of the eukaryal V-ATPases. This is a clear example for a structural change leading to a fundamental functional difference in the ATPases. Of course, when the  $\Delta p$  is increased artificially, the driving force is increased, and

the enzyme is forced to synthesize ATP even at a  $H^+$ /ATP stoichiometry of 2. This has been demonstrated recently for the V-ATPase from yeast [157].

These two examples clearly define the two extremes, but what is the minimal number of ions allowing ATP synthesis? Again, of course, this is dependent on the energetic parameters  $\Delta G_p$  and  $\Delta p$ . However, two recent examples may be used to narrow down this number. The bacterium *A. woodii* contains at least one copy of the 16-kDa proteolipid in the  $c$  oligomer, which gives a maximal number of 11 ion-translocating residues or a maximal ion/ATP stoichiometry of 3.6 for ATP synthesis [66]. The archaeon *M. jannaschii* has a triplicated proteolipid with only 2 ion-translocating groups. Apparently, 2.6 carboxyl groups per catalytic center are already sufficient for ATP synthesis [134].

### A new layer of regulation of ATPases?

As pointed out above, the number of ions translocated per catalytic center is an important parameter in determining the direction of the reaction catalyzed by ATPases. So far, we have seen that V-ATPases evolved a proteolipid oligomer with only half the amount of ion-translocating groups, which prevents ATP synthesis but promotes ion pumping. Accordingly, it should be possible to switch between ATP synthesis or ATP hydrolysis in F/A-ATPases by changing the number of ion-translocating groups per  $c$  oligomer. Clearly, it is hard to envisage how the number of ion-translocating groups in a given oligomer could be changed, but it seems feasible to alter the number of monomers or the composition of the  $c$  oligomer at the level of assembly. This was originally suggested by Brusilow and co-workers based on experimental data obtained with *E. coli* [158], but might also be true for *A. woodii* with its 8- and 16-kDa proteolipids. *E. coli* was shown to have a higher number of  $c$  subunits during growth on glucose compared with growth on succinate [158]. *A. woodii* can switch from ion gradient-driven phosphorylation to fermentation, and under fermentative conditions the ATP synthase should work as an ATP-driven ion pump to generate the  $\Delta\mu_{ion}$  across the cytoplasmic membrane that is essential to any living cell (fig. 8). Regulation of the number of  $c$  subunits per  $c$  oligomer could turn out to be a new regulatory mechanism in ATPases. Unfortunately, an experimental setup to approach this interesting, potentially new layer of regulation of ATPases experimentally is hampered by technical difficulties.

### Evolution of ATPases

The same structure of two domains connected by one (or two) stalk(s) is found in ATPases from all three branches of the evolutionary tree, and it is assumed that all AT-

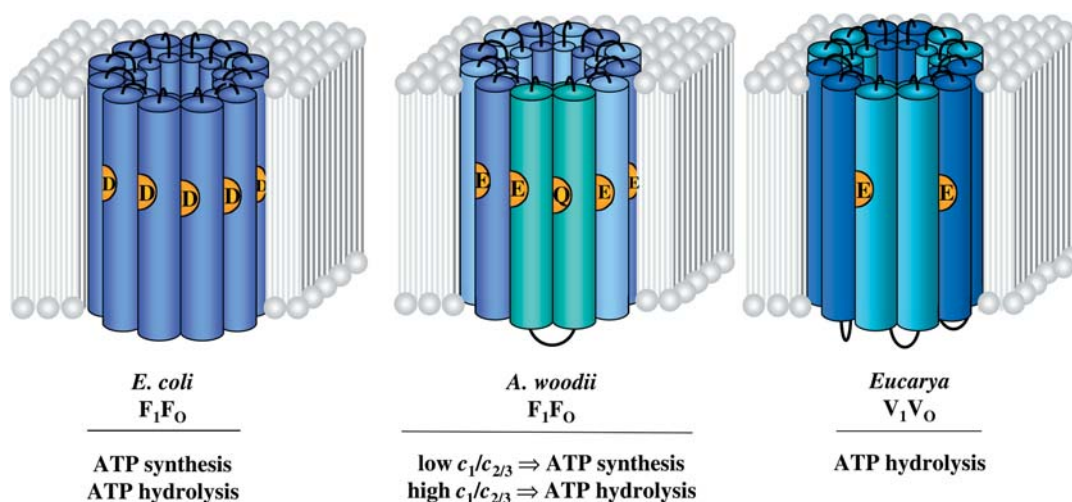


Figure 8. Regulation of ATPases by changing the proteolipid stoichiometries. Indicated are the proteolipid oligomers each having 24 trans-membrane helices. This is made from 12 monomers in *E. coli* F<sub>1</sub>F<sub>0</sub>-ATPase or 6 monomers in eukaryal V<sub>1</sub>V<sub>0</sub>-ATPases. The stoichiometry of the 16- ( $c_1$ ) and 8-kDa proteolipids ( $c_2/c_3$ ) in *A. woodii* is unknown. For explanations, see text.

Pases arose from a common ancestor [159, 160]. The major polypeptides ( $\alpha$  and  $\beta$ , A and B) originated from duplication of one ancestral gene. In the line leading to the A<sub>1</sub>A<sub>0</sub>/V<sub>1</sub>V<sub>0</sub>-ATPases, a number of deletions and insertions occurred which on the one hand led to the loss of catalytic activity from one subunit of the A<sub>3</sub>B<sub>3</sub> core particle, which still needs to bind nucleotides in order to achieve its proper folding, and on the other hand to an enlargement of the catalytic subunit relative to the noncatalytic which is vice versa in F<sub>1</sub>F<sub>0</sub>-ATPases.

Phylogenetic analyses of subunit A clearly revealed that F<sub>1</sub>F<sub>0</sub>-, A<sub>1</sub>A<sub>0</sub>- and V<sub>1</sub>V<sub>0</sub>-ATPases form separate clusters and agree well with analyses based on 16S ribosomal RNA (rRNA) sequences [161]. Thus, it appears that the ATPases have evolved together with the organisms that they reside in. Therefore, the term 'V<sub>1</sub>V<sub>0</sub>-ATPases' should be restricted to eukaryal ATPases and not be used for archaeal ATPases, as is often done. The ATPases from *Thermus thermophilus* HB27 and *E. hirae* are always referred to as V-ATPases, although phylogenetic analyses clearly show that they cluster within the A-ATPases [18]. They are of archaeal origin and should not be considered as V<sub>1</sub>V<sub>0</sub>- but as A<sub>1</sub>A<sub>0</sub>-ATPases! This is a very important finding, as it can be taken as evidence for horizontal transfer of genes involved in central metabolism between domains. In fact, representatives of the genus *Thermus* are known for their extremely high competence for natural transformation, i.e. uptake of naked DNA [162, 163]. That shuffling of large pieces of DNA occurred during early evolution is also evident from the fact that 30% of the genes of the mesophilic archaeon *M. mazei* are of bacterial origin.

The majority of bacteria have F-ATPases, and the majority of archaea A-ATPases. However, there are exceptions. Two archaeal species, *M. barkeri* and *M. acetivorans*,

have in addition to the A-ATPase genes an F-ATPase gene cluster encoding the eight structural subunits of bacterial F-ATPases [122, 123]. However, to date there is no indication that these F-ATPase genes are transcribed or that an F-ATPase is produced in addition to the A-ATPase [T. Lemker and V. Müller, unpublished]. The anaerobic, fermenting Gram-positive bacterium *E. hirae* has an F-type ATPase to energize the cytoplasmic membrane, and a Na<sup>+</sup>-translocating A[V]-type ATPase which is induced at alkaline pH [164].

There was always the hypothesis that the diversion of the A<sub>1</sub>A<sub>0</sub>- and V<sub>1</sub>V<sub>0</sub>-ATPases took place by a duplication and subsequent fusion of the genes encoding the proteolipid [165]. However, it appears that this is not the case based on the following evidence (Fig. 9). Two genes each encoding a 8-kDa proteolipid are present in the archaeon *Archaeoglobus fulgidus*, which apparently represents an intermediate in evolution [166]. Duplicated and even triplicated proteolipid-encoding genes that arose by multiplication events followed by fusion of the gene products were recently found in the A<sub>1</sub>A<sub>0</sub>-ATP synthases from *M. thermoautotrophicus* and *M. jannaschii*, respectively [134, 135]. This first evidence for multiplied proteolipids in A<sub>1</sub>A<sub>0</sub>-ATPases shook the dogma of '16-kDa proteolipids in V-ATPases only'. Interestingly, these multiplied proteolipids, were not 'typical' V-type proteolipids, for the ion-translocating group was conserved in every hairpin (*M. thermoautotrophicus*) or in two out of three (*M. jannaschii*). However, 'typical' 16-kDa proteolipids with the ion-translocating group conserved only in TM2 are present in members of the archaeal genus *Pyrococcus*, as deduced from the genome sequence of two strains [167], but the major subunits clearly cluster within the A<sub>1</sub>A<sub>0</sub>-ATPases. Therefore, this seems to be the first A<sub>1</sub>A<sub>0</sub>-ATPase with a typical 'eukaryal' 16-kDa proteolipid. How

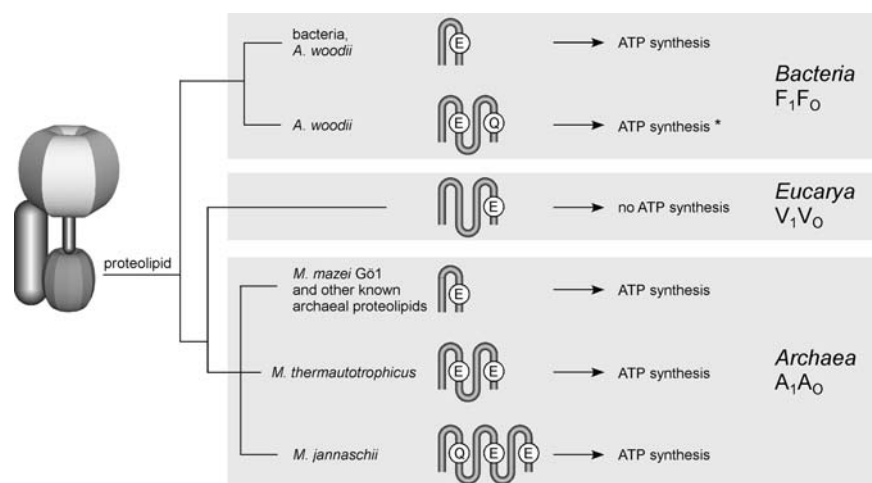


Figure 9. Evolution of structure and function of ATPases. The evolution of the ATPases is delineated from their major subunits. In addition, the structure of the proteolipids and the function of the enzymes are given. \*Please note that *A. woodii* does not have the 16-kDa proteolipid only but a mixture of 8- and 16-kDa proteolipids ( $c_1$  and  $c_2/c_3$ ).

can this finding be explained? From what is known to date, the metabolism of *Pyrococcus* seems to be exclusively fermentative [168]. ATP is generated by substrate level phosphorylation, and the cytoplasmic membrane is energized by action of the A-ATPase. Evolution evidently drove the production of an  $A_1A_0$ -ATPase with a 16-kDa proteolipid having only six ion-translocating groups per  $c$  oligomer. As in the case of  $V_1V_0$ -ATPases, this enzyme is well designed as an ion pump to energize the cytoplasmic membrane. It should be mentioned in this context that it was speculated that the switch from a A- to a V-type ATPase occurred after an archaeon had picked up a bacterial symbiont on the way to becoming an eukaryote [169]. However, in light of the finding of V-like proteolipids in *Pyrococcus*, this switch must have occurred earlier and could have been driven by a loss of the ability of ion gradient-driven phosphorylation. *Pyrococcus* or its ancestors might be descendents of the archaeal host that gave rise to eukaryotes.

Most recently, the first  $F_1F_0$ -ATPase having a mixed oligomer of two identical 8- and one 16-kDa proteolipid with only one ion-translocating group in four TM helices was found in the bacterium *A. woodii* [69]. These subunits are encoded by three genes embedded into the  $F_1F_0$ -ATPase operon. *atpE<sub>2</sub>* and *atpE<sub>3</sub>* are 100% identical on the amino acid level, and *atpE<sub>1</sub>* arose by duplication of an ancestral gene with subsequent fusion of the two gene copies. This is the first example of a  $F_1F_0$ -ATPase having, in addition to bacterial 8-kDa proteolipids, a V-like proteolipid, again, showing that 16-kDa proteolipids are not restricted to V-type ATPases.

In summary, duplication events leading to multiplied proteolipids are no exclusive feature of  $V_1V_0$ -ATPases but occurred in all three lines of descent (fig. 9). Therefore, this is not a valid criterium to distinguish V- and A-AT-

Pases. Multiplication events in the proteolipid-encoding gene a priori are of no consequence for the function of the enzyme. This is also corroborated by the finding that genetically engineered duplicated versions of the proteolipid of the *E. coli*  $F_1F_0$ -ATP synthase allows growth of *E. coli* on a nonfermentable carbon source [170]. The important point is the number of protonizable groups in the subunit  $c$  oligomer, as pointed out above. For certain organisms and organelles it was advantageous to reduce the number of ion-translocating groups, thus making the enzyme a better ion pump; however, this had happened independently in all three lines of descent.

What could be the selective pressure for multiplication of proteolipid-encoding genes? One has to keep in mind that the subunits of the ATPase are present in different stoichiometries ( $a_1b_2c_{9-14}\delta\alpha_3\gamma\beta_3\epsilon$ ), and the proteolipid (subunit  $c$ ) has by far the highest copy number in the complex. Most of our knowledge concerning the regulation of the synthesis of the proteolipid derived from the paradigm *E. coli*. There, the proteolipid-encoding gene is part of a polycistronic message, and enhanced synthesis of the proteolipid is achieved by enhancement of translation [171]. In addition, but to a lesser extent, regulation by differential messenger RNA (mRNA) stability contributes to differential gene expression [172]. Apparently, multiplication of the *atpE* gene and embedding the copies into the operon is another way to increase the concentration of subunit  $c$ . This strategy is apparently realized by *A. woodii*, eukarya and some archaea [67, 173].

## Concluding remarks

A-/F-/V-ATPases are fascinating enzymes that arose from a common ancestor and are present in every life

form. They are essential for life and known as the coupling factors that convert the electrochemical ion gradient across the membrane to the synthesis of ATP and vice versa. Molecular and biochemical studies revealed a complex subunit composition of the enzymes, and recent studies gave fantastic insights into the three-dimensional structure of F-ATPases. These enzymes work as molecular rotational motors, the smallest found in biology. This finding stimulates the imagination of many researchers engaged in the production of motors on a nanometer scale. The study of V- and A-ATPases is lagging behind, but there is reason to hope that high-resolution structures of these enzymes and mechanistic studies will follow soon. These studies will build the foundation on which to base questions addressing the role of subunits found only in V- and A-ATPases and their relation to specific functions of the enzymes. The overall structure of the ATPases as well as their catalytic properties, ion transport and coupling mechanism have been well conserved during evolution, and therefore results obtained from the study of one enzyme can often be generalized. The study of enzymes from nonstandard organisms will continue to deepen our understanding of the structure and function of these enzymes. The best example is probably the finding of Na<sup>+</sup>-translocating ATPases that offer a different way to approach rotor function and coupling mechanisms. Due to the fascinating variability of the physiology of archaea and their life in extreme habitats, we see a variation in structure and function of archaeal ATPases. Proteolipids that arose by gene duplication and triplication events have been already discovered, but perhaps we will see higher degrees of multiplication in the future. In the future, we also expect to find different ion specificities of A<sub>1</sub>A<sub>0</sub>-ATPases, as already observed in F<sub>1</sub>F<sub>0</sub>-ATPases.

**Acknowledgements.** The authors are indebted to their co-workers for their excellent work and to Dr. Lemker for the art work. Research from the authors laboratory was supported by grants from the Deutsche Forschungsgemeinschaft (MU 801/10-2 and GR 1475/9-1).

- 1 Stock D., Gibbons C., Arechaga I., Leslie A. G. and Walker J. E. (2000) The rotary mechanism of ATP synthase. *Curr. Opin. Struct. Biol.* **10**: 672–679
- 2 Buchanan S. K. and Walker J. E. (1996) Large-scale chromatographic purification of F<sub>1</sub>F<sub>0</sub>-ATPase and complex I from bovine heart mitochondria. *Biochem. J.* **318**: 343–349
- 3 Müller V., Ruppert C. and Lemker T. (1999) Structure and function of the A<sub>1</sub>A<sub>0</sub> ATPases from methanogenic archaea. *J. Bioenerg. Biomembr.* **31**: 15–28
- 4 Mitchell P. (1961) Coupling of phosphorylation to electron and hydrogen transfer by a chemiosmotic mechanism. *Nature* **191**: 144–148
- 5 Graham L. A., Powell B. and Stevens T. H. (2000) Composition and assembly of the yeast vacuolar H<sup>+</sup>-ATPase complex. *J. Exp. Biol.* **203**: 61–70
- 6 Kasho V. N. and Boyer P. D. (1989) Vacuolar ATPases, like F<sub>1</sub>,F<sub>0</sub>-ATPases, show a strong dependence of the reaction velocity on the binding of more than one ATP per enzyme. *Proc. Natl. Acad. Sci. USA* **86**: 8708–8711
- 7 Uchida E., Ohsumi Y. and Anraku Y. (1988) Characterization and function of catalytic subunit alpha of H<sup>+</sup>-translocating adenosine triphosphatase from vacuolar membranes of *Saccharomyces cerevisiae*. A study with 7-chloro-4-nitrobenzo-2-oxa-1,3-diazole. *J. Biol. Chem.* **263**: 45–51
- 8 Hanada H., Moriyama Y., Maeda M., and Futai M. (1990) Kinetic studies of chromaffin granule H<sup>+</sup>-ATPase and effects of bafilomycin A<sub>1</sub>. *Biochem. Biophys. Res. Commun.* **170**: 873–878
- 9 Futai M., Omote H., Sambongi Y. and Wada Y. (2000) Syn- thase (H<sup>+</sup> ATPase): coupling between catalysis, mechanical work, and proton translocation. *Biochim. Biophys. Acta* **1458**: 276–288
- 10 Nishi T. and Forgacs M. (2002) The vacuolar H<sup>+</sup>-ATPases – Nature's most versatile proton pumps. *Nat. Rev. Mol. Cell. Biol.* **3**: 94–103
- 11 Grüber G., Wiczorek H., Harvey W. R. and Müller V. (2001) Structure-function relationships of A-, F- and V-ATPases. *J. Exp. Biol.* **204**: 2597–2605
- 12 Wilkens S. and Capaldi R. A. (1998) Electron microscopic evidence of two stalks linking the F<sub>1</sub> and F<sub>0</sub> parts of the *Escherichia coli* ATP synthase. *Biochim. Biophys. Acta* **1365**: 93–97
- 13 Karrasch S. and Walker J. E. (1999) Novel features in the structure of bovine ATP synthase. *J. Mol. Biol.* **290**: 379–384
- 14 Boekema E. J., Ubbink-Kok T., Lolkema J. S., Brisson A. and Konings W. N. (1997) Visualization of a peripheral stalk in V-type ATPase: evidence for the stator structure essential for rotational catalysis. *Proc. Natl. Acad. Sci. USA* **94**: 14291–14293
- 15 Domgall I., Venzke D., Lüttge U., Ratajczak R. and Böttcher B. (2002) Three-dimensional map of a plant V-ATPase based on electron microscopy. *J. Biol. Chem.* **277**: 13115–13121
- 16 Pedersen P. L., Ko Y. H. and Hong S. (2000) ATP synthases in the year 2000: evolving views about the structures of these remarkable enzyme complexes. *J. Bioenerg. Biomembr.* **32**: 325–332
- 17 Yoshida M., Muneyuki E. and Hisabori T. (2001) ATP synthase-a marvellous rotary engine of the cell. *Nat. Rev. Mol. Cell. Biol.* **2**: 669–677
- 18 Hilario E. and Gogarten J. P. (1998) The prokaryote-to-eucaryote transition reflected in the evolution of the V/F/A-ATPase catalytic and proteolipid subunits. *J. Mol. Evol.* **46**: 703–715
- 19 Boyer P. D. (1993) The binding change mechanism for ATP synthase – some probabilities and possibilities. *Biochim. Biophys. Acta* **1140**: 215–250
- 20 Schäfer H. J. and Dose K. (1984) Photoaffinity cross-linking of the coupling factor 1 from *Micrococcus luteus* by 3'-arylazido-8-azido-ATP. *J. Biol. Chem.* **259**: 15301–15306
- 21 Gresser M. J., Myers J. A. and Boyer P. D. (1982) Catalytic site cooperativity of beef heart mitochondrial F<sub>1</sub> adenosine triphosphatase. Correlations of initial velocity, bound intermediate and oxygen exchange measurements with an alternating three-site model. *J. Biol. Chem.* **257**: 12030–12038
- 22 Weber J. and Senior A. E. (2000) ATP synthase: what we know about ATP hydrolysis and what we do not know about ATP synthesis. *Biochim. Biophys. Acta* **1458**: 300–309
- 23 Grüber G. and Capaldi R. A. (1996) Differentiation of catalytic sites on *Escherichia coli* F<sub>1</sub> ATPase by laser photoactivated labeling with [H-3]-2-azido-ATP using the mutant βGlu381Cys:εSer108Cys to identify different β subunits by their interactions with γ and ε subunits. *Biochemistry* **35**: 3875–3879
- 24 Weber J. and Senior A. E. (1996) Binding and hydrolysis of TNP-ATP by *Escherichia coli* F<sub>1</sub>-ATPase. *J. Biol. Chem.* **271**: 3474–3477



- 25 Abrahams J. P., Leslie A. G. W., Lutter R. and Walker J. E. (1994) Structure at 2.8 Å resolution of F<sub>1</sub>-ATPase from bovine heart mitochondria. *Nature* **370**: 621–628
- 26 Leslie A. G. and Walker J. E. (2000) Structural model of F<sub>1</sub>-ATPase and the implications for rotary catalysis. *Philos. Trans. R. Soc. Lond. B. Biol. Sci.* **355**: 465–471
- 27 Menz R. I., Walker J. E. and Leslie A. G. (2001) Structure of bovine mitochondrial F<sub>1</sub>-ATPase with nucleotide bound to all three catalytic sites: implications for the mechanism of rotary catalysis. *Cell* **106**: 331–341
- 28 Bianchet M. A., Hüllihen J., Pedersen P. L. and Amzel M. L. (1998) The 2.8-Å structure of rat liver F<sub>1</sub> ATPase: configuration of a critical intermediate in ATP synthesis/hydrolysis. *Proc. Natl. Acad. Sci. USA* **95**: 11065–11070
- 29 Groth G. and Pohl E. (2001) The structure of the chloroplast F<sub>1</sub>-ATPase at 3.2 Å resolution. *J. Biol. Chem.* **276**: 1345–1352
- 30 Hausrath A. C., Grüber G., Matthews B. W. and Capaldi R. A. (1999) Structural features of the  $\gamma$  subunit of the *Escherichia coli* F<sub>1</sub> ATPase revealed by a 4.4-Å resolution map obtained by X-ray crystallography. *Proc. Natl. Acad. Sci. USA* **96**: 13697–13702
- 31 Rodgers A. J. and Wilce M. C. (2000) Structure of the  $\gamma/\epsilon$  complex of ATP synthase. *Nat. Struct. Biol.* **7**: 1051–1054
- 32 Gibbons C., Montgomery M. G., Leslie A. G. and Walker J. E. (2000) The structure of the central stalk in bovine F<sub>1</sub>-ATPase at 2.4 Å resolution. *Nat. Struct. Biol.* **7**: 1055–1061
- 33 Watts S. D., Zhang Y., Fillingame R. H. and Capaldi R. A. (1995) The  $\gamma$  subunit in the *Escherichia coli* ATP synthase complex (ECF<sub>1</sub>F<sub>0</sub>) extends through the stalk and contacts the *c* subunits of the F<sub>0</sub> part. *FEBS Lett.* **368**: 235–238
- 34 Watts S. D., Tang C. L. and Capaldi R. A. (1996) The stalk region of the *Escherichia coli* ATP synthase – Tyrosine 205 of the  $\gamma$  subunit is in the interface between the F<sub>1</sub> and F<sub>0</sub> parts and can interact with both the  $\epsilon$  and *c* oligomer. *J. Biol. Chem.* **271**: 28341–28347
- 35 Stock D., Leslie A. G. and Walker J. E. (1999) Molecular architecture of the rotary motor in ATP synthase. *Science* **286**: 1700–1705
- 36 Uhlin U., Cox G. B. and Guss J. M. (1997) Crystal structure of the  $\epsilon$  subunit of the proton-translocating ATP synthase from *Escherichia coli*. *Structure* **5**: 1219–1230
- 37 Hausrath A. C., Capaldi R. A. and Matthews B. W. (2001) The conformation of the  $\epsilon/\gamma$ -subunits within the *Escherichia coli* F<sub>1</sub> ATPase. *J. Biol. Chem.* **276**: 47227–47232
- 38 Tsunoda S. P., Rodgers A. J., Aggeler R., Wilce M. C., Yoshida M. and Capaldi R. A. (2001) Large conformational changes of the  $\epsilon$  subunit in the bacterial F<sub>1</sub>F<sub>0</sub> ATP synthase provide a ratchet action to regulate this rotary motor enzyme. *Proc. Natl. Acad. Sci. USA* **98**: 6560–6564
- 39 Dmitriev O., Jones P. C., Jiang W. and Fillingame R. H. (1999) Structure of the membrane domain of subunit *b* of the *Escherichia coli* F<sub>0</sub>F<sub>1</sub> ATP synthase. *J. Biol. Chem.* **274**: 15598–15604
- 40 Dunn S. D. (1992) The polar domain of the *b* subunit of *Escherichia coli* F<sub>1</sub>F<sub>0</sub>-ATPase forms an elongated dimer that interacts with the F<sub>1</sub> sector. *J. Biol. Chem.* **267**: 7630–7636
- 41 Böttcher B. and Grüber P. (2000) The structure of the H<sup>+</sup>-ATP synthase from chloroplasts and its subcomplexes as revealed by electron microscopy. *Biochim. Biophys. Acta* **1458**: 404–416
- 42 Del Rizzo P. A., Bi Y., Dunn S. D. and Shilton B. H. (2002) The second stalk of *Escherichia coli* ATP synthase: structure of the isolated dimerization domain. *Biochemistry* **41**: 6875–6884
- 43 Cain B. D. (2000) Mutagenic analysis of the F<sub>0</sub> stator subunits. *J. Bioenerg. Biomembr.* **32**: 365–371
- 44 Jiang W. and Fillingame R. H. (1998) Interacting helical faces of subunits *a* and *c* in the F<sub>1</sub>F<sub>0</sub> ATP synthase of *Escherichia coli* defined by disulfide cross-linking. *Proc. Natl. Acad. Sci. USA* **95**: 6607–6612
- 45 Turina P. and Melandri B. A. (2002) A point mutation in the ATP synthase of *Rhodobacter capsulatus* results in differential contributions of  $\Delta pH$  and  $\Delta\Psi$  in driving the ATP synthesis reaction. *Eur. J. Biochem.* **269**: 1984–1992
- 46 Valiyaveetil F. I. and Fillingame R. H. (1997) On the role of Arg-210 and Glu-219 of subunit *a* in proton translocation by the *Escherichia coli* F<sub>0</sub>F<sub>1</sub>-ATP synthase. *J. Biol. Chem.* **272**: 32635–32641
- 47 Vik S. B. and Antonio B. J. (1994) A mechanism of proton translocation by F<sub>1</sub>F<sub>0</sub> ATP synthases suggested by double mutants of the *a* subunit. *J. Biol. Chem.* **269**: 30364–30369
- 48 Wada T., Long J. C., Zhang D. and Vik S. B. (1999) A novel labeling approach supports the five-transmembrane model of subunit *a* of the *Escherichia coli* ATP synthase. *J. Biol. Chem.* **274**: 17353–17357
- 49 Valiyaveetil F. I. and Fillingame R. H. (1998) Transmembrane topography of subunit *a* in the *Escherichia coli* F<sub>1</sub>F<sub>0</sub> ATP synthase. *J. Biol. Chem.* **273**: 16241–16247
- 50 Jäger H., Birkenhäger R., Stalz W.-D., Altendorf K. and Deckers-Hebestreit G. (1998) Topology of subunit *a* of the *Escherichia coli* ATP synthase. *Eur. J. Biochem.* **251**: 122–132
- 51 Fillingame R. H., Jiang W. and Dmitriev O. Y. (2000) Coupling H<sup>+</sup> transport to rotary catalysis in F-type ATP synthases: structure and organization of the transmembrane rotary motor. *J. Exp. Biol.* **203**: 9–17
- 52 Altendorf K., Stalz W., Greie J. and Deckers-Hebestreit G. (2000) Structure and function of the F<sub>0</sub> complex of the ATP synthase from *Escherichia coli*. *J. Exp. Biol.* **203**: 19–28
- 53 Rastogi V. K. and Girvin M. E. (1999) Structural changes linked to proton translocation by subunit *c* of the ATP synthase. *Nature* **402**: 263–268
- 54 Stahlberg H., Müller D. J., Suda K., Fotiadis D., Engel A., Meier T. et al. (2001) Bacterial Na<sup>+</sup>-ATP synthase has an undecameric rotor. *EMBO Rep.* **2**: 229–233
- 55 Vonck J., v. Nidda T. K., Meier T., Matthey U., Mills D. J., Kühlbrandt W., et al. (2002) Molecular architecture of the undecameric rotor of a bacterial Na<sup>+</sup>-ATP synthase. *J. Mol. Biol.* **321**, 307–316
- 56 Seelert H., Poetsch A., Dencher N. A., Engel A., Stahlberg H. and Müller D. J. (2000) Structural biology. Proton-powered turbine of a plant motor. *Nature* **405**: 418–419
- 57 Jones P. C., Jiang W. and Fillingame R. H. (1998) Arrangement of the multicopy H<sup>+</sup>-translocating subunit *c* in the membrane sector of the *Escherichia coli* F<sub>1</sub>F<sub>0</sub> ATP synthase. *J. Biol. Chem.* **273**: 17178–17185
- 58 Fillingame R. H., Jiang W., Dmitriev O. Y. and Jones P. C. (2000) Structural interpretations of F<sub>0</sub> rotary function in the *Escherichia coli* F<sub>1</sub>F<sub>0</sub> ATP synthase. *Biochim. Biophys. Acta* **1458**: 387–403
- 59 Groth G. and Walker J. E. (1997) Model of the *c*-subunit oligomer in the membrane domain of F-ATPases. *FEBS Lett.* **410**: 117–123
- 60 Schnick C., Forrest L. R., Sansom M. S. and Groth G. (2000) Molecular contacts in the transmembrane *c*-subunit oligomer of F-ATPases identified by tryptophan substitution mutagenesis. *Biochim. Biophys. Acta* **1459**: 49–60
- 61 Junge W., Lill H. and Engelbrecht S. (1997) ATP synthase: an electrochemical transducer with rotatory mechanics. *Trends Biochem. Sci.* **22**: 420–423
- 62 Dimroth P., Matthey U. and Kaim G. (2000) Critical evaluation of the one- versus the two-channel model for the operation of the ATP synthase's motor. *Biochim. Biophys. Acta* **1459**: 506–513
- 63 Matthey U., Braun D. and Dimroth P. (2002) NMR investigations of subunit *c* of the ATP synthase from *Propionigenium modestum* in chloroform/methanol/water (4:4:1). *Eur. J. Biochem.* **269**: 1942–1946
- 64 von Ballmoos C., Appoldt Y., Brunner J., Granier T., Vasella A. and Dimroth P. (2002) Membrane topography of the coupling

- ion binding site in Na<sup>+</sup>-translocating F<sub>1</sub>F<sub>0</sub> ATP synthase. J. Biol. Chem. **277**: 3504–3510
- 65 Birkenhäger R., Hoppert M., Deckers-Hebestreit G., Mayer F. and Altendorf K. (1995) The F<sub>0</sub> complex of the *Escherichia coli* ATP synthase – investigation by electron spectroscopic imaging and immunoelectron microscopy. Eur. J. Biochem. **230**: 58–67
  - 66 Singh S., Turina P., Bustamante C. J., Keller D. J. and Capaldi R. (1996) Topographical structure of membrane-bound *Escherichia coli* F<sub>1</sub>F<sub>0</sub> ATP synthase in aqueous buffer. FEBS Lett. **397**: 30–34
  - 67 Rahlfs S., Aufurth S. and Müller V. (1999) The Na<sup>+</sup>-F<sub>1</sub>F<sub>0</sub>-ATPase operon from *Acetobacterium woodii*. Operon structure and presence of multiple copies of *atpE* which encode proteolipids of 8- and 18-kDa. J. Biol. Chem. **274**: 33999–34004
  - 68 Aufurth S., Schägger H. and Müller V. (2000) Identification of subunits *a*, *b*, and *c*<sub>1</sub> from *Acetobacterium woodii* Na<sup>+</sup>-F<sub>1</sub>F<sub>0</sub>-ATPase. Subunits *c*<sub>1</sub>, *c*<sub>2</sub>, and *c*<sub>3</sub> constitute a mixed *c*-oligomer. J. Biol. Chem. **275**: 33297–33301
  - 69 Müller V., Aufurth S. and Rahlfs S. (2001) The Na<sup>+</sup> cycle in *Acetobacterium woodii*: identification and characterization of a Na<sup>+</sup> translocating F<sub>1</sub>F<sub>0</sub>-ATPase with a mixed oligomer of 8- and 16-kDa proteolipids. Biochim. Biophys. Acta **1505**: 108–120
  - 70 Dimroth P. (1997) Primary sodium ion translocating enzymes. Biochim. Biophys. Acta **1318**: 11–51
  - 71 Zhang Y. and Fillingame R. H. (1995) Changing the ion binding specificity of the *Escherichia coli* H<sup>+</sup>-transporting ATP synthase by directed mutagenesis of subunit *c*. J. Biol. Chem. **270**: 87–93
  - 72 Kaim G., Wehrle F., Gerike U. and Dimroth P. (1997) Molecular basis for the coupling ion selectivity of F<sub>1</sub>F<sub>0</sub> ATP synthases: probing the liganding groups for Na<sup>+</sup> and Li<sup>+</sup> in the *c* subunit of the ATP synthase from *Propionigenium modestum*. Biochemistry **36**: 9185–9194
  - 73 Rahlfs S. and Müller V. (1997) Sequence of subunit *c* of the Na<sup>+</sup>-translocating F<sub>1</sub>F<sub>0</sub> ATPase of *Acetobacterium woodii*: proposal for determinants of Na<sup>+</sup> specificity as revealed by sequence comparisons. FEBS Lett. **404**: 269–271
  - 74 Rahlfs S. and Müller V. (1999) Sequence of subunit *a* of the Na<sup>+</sup>-translocating F<sub>1</sub>F<sub>0</sub>-ATPase of *Acetobacterium woodii*: proposal for residues involved in Na<sup>+</sup> binding. FEBS Lett. **453**: 35–40
  - 75 Sumner J. P., Dow J. A. T., Earley F. G., Klein U., Jäger D. and Wiczorek H. (1995) Regulation of plasma membrane V-ATPase activity by dissociation of peripheral subunits. J. Biol. Chem. **270**: 5649–5653
  - 76 Kane P. M. (1995) Disassembly and reassembly of the yeast vacuolar H<sup>+</sup>-ATPase in vivo. J. Biol. Chem. **270**: 17025–17032
  - 77 Kane P. M. (2000) Regulation of V-ATPase by reversible disassembly. FEBS Lett. **469**: 137–141
  - 78 Wiczorek H., Grüber G., Harvey W. R., Huss M., Merzen-dorfer H. and Zeiske W. (2000) Structure and regulation of insect plasma membrane H<sup>+</sup> V-ATPase. J. Exp. Biol. **203**: 127–135
  - 79 Gräf R., Harvey W. R. and Wiczorek H. (1996) Purification and properties of a cytosolic V<sub>1</sub>-ATPase. J. Biol. Chem. **271**: 20908–20913
  - 80 Svergun D. I., Konrad S., Huss M., Koch M. H., Wiczorek H., Altendorf K. et al. (1998) Quaternary structure of V<sub>1</sub> and F<sub>1</sub> ATPase: significance of structural homologies and diversities. Biochemistry **37**: 17659–17663
  - 81 Xu T., Vasilyeva E. and Forgac M. (1999) Subunit interactions in the clathrin-coated vesicle vacuolar H<sup>+</sup>-ATPase complex. J. Biol. Chem. **274**: 2890–28915
  - 82 Boekema E. J., Ubbink-Kok T., Lolkema J. S., Brisson A. and Konings W. N. (1998) Structure of V-type ATPase from *Clostridium fervidus* by electron microscopy. Photosyn. Research **57**: 267–273
  - 83 Radermacher M., Ruiz T., Harvey W. R., Wiczorek H. and Grüber G. (1999) Molecular architecture of *Manduca sexta* midgut V<sub>1</sub> ATPase visualized by electron microscopy. FEBS Lett. **453**: 383–386
  - 84 Grüber G., Radermacher M., Ruiz T., Godovac-Zimmermann J., Canas B., Kleine-Kohlbrecher D. et al. (2000) Three-dimensional structure and subunit topology of the V<sub>1</sub> ATPase from *Manduca sexta* midgut. Biochemistry **39**: 8609–8616
  - 85 Radermacher M., Ruiz T., Wiczorek H. and Grüber G. (2001) The structure of the V<sub>1</sub>-ATPase determined by three-dimensional electron microscopy of single particles. J. Struct. Biol. **135**: 26–37
  - 86 Wilkens S., Vasilyeva E. and Forgac M. (1999) Structure of the vacuolar ATPase by electron microscopy. J. Biol. Chem. **274**: 31804–31810
  - 87 Grüber G., Svergun D. I., Coskun Ü., Lemker T., Koch M. H., Schägger H. et al. (2001) Structural insights into the A<sub>1</sub> ATPase from the archaeon, *Methanosarcina mazei* Gö1. Biochemistry **40**: 189–1896
  - 88 Sagermann M., Stevens T. H. and Matthews B. W. (2001) Crystal structure of the regulatory subunit H of the V-type ATPase of *Saccharomyces cerevisiae*. Proc. Natl. Acad. Sci. USA **98**: 7134–7139
  - 89 Tomashek J. J., Graham L. A., Hutchins M. U., Stevens T. H. and Klionsky D. J. (1997) V<sub>1</sub>-situated stalk subunits of the yeast vacuolar proton-translocating ATPase. J. Biol. Chem. **272**: 2678–26793
  - 90 Lu M., Vergara S., Zhang L., Holliday L. S., Aris J., and Gluck S. L. (2002) The amino-terminal domain of the E-subunit of V-ATPase interacts with the H subunit and is required for V-ATPase function. J. Biol. Chem. **277**: 38409–38415
  - 91 Xu T., Vasilyeva E. and Forgac M. (1999) Subunit interaction in the clathrin-coated vesicle vacuolar (H<sup>+</sup>)-ATPase complex. J. Biol. Chem. **274**: 28909–28915
  - 92 Nelson H., Mandiyan S. and Nelson N. (1995) A bovine cDNA and a yeast gene (VMA8) encoding the subunit D of the vacuolar H<sup>+</sup>-ATPase. Proc. Natl. Acad. Sci. USA **92**: 497–501
  - 93 Arata Y., Baleja J. D. and Forgac M. (2002) Cysteine-directed cross-linking to subunit B suggests that subunit E forms part of the peripheral stalk of the vacuolar H<sup>+</sup>-ATPase. J. Biol. Chem. **277**: 3357–3363
  - 94 Bowman E. J., Steinhardt A. and Bowman B. J. (1995) Isolation of the *vma-4* gene encoding the 26 kDa subunit of the *Neurospora crassa* vacuolar ATPase. Biochim. Biophys. Acta **1237**: 95–98
  - 95 Schäfer H. J., Coskun Ü., Eger O., Godovac-Zimmermann J., Wiczorek H., Kagawa Y. et al. (2001) 8-N<sub>3</sub>-3'-biotinyl-ATP, a novel monofunctional reagent: differences in the F<sub>1</sub>- and V<sub>1</sub>-ATPases by means of the ATP analogue. Biochem. Biophys. Res. Commun. **286**: 1218–1227
  - 96 Xie X. S. (1996) Reconstitution of ATPase activity from individual subunits of the clathrin-coated vesicle proton pump – the requirement and effect of three small subunits. J. Biol. Chem. **271**: 30980–30985
  - 97 Peng S. B., Zhang Y., Tsai S. J., Xie X. S. and Stone D. K. (1994) Reconstitution of recombinant 33-kDa subunit of the clathrin-coated vesicle H<sup>+</sup>-ATPase. J. Biol. Chem. **269**: 11356–11360
  - 98 Boekema E. J., van Breemen J. F., Brisson A., Ubbink-Kok T., Konings W. N. and Lolkema J. S. (1999) Connecting stalks in V-type ATPase. Nature **401**: 37–38
  - 99 Kawasaki-Nishi S., Nishi T. and Forgac M. (2001) Arg-735 of the 100 kDa subunit *a* of the yeast V-ATPase is essential for proton translocation. Proc. Natl. Acad. Sci. USA **98**: 12397–12402
  - 100 Landolt-Marticorena C., Williams K. M., Correa J., Chen W. and Manolson M. F. (2000) Evidence that the NH<sub>2</sub>-terminus of vph1p, an integral subunit of the V<sub>0</sub> sector of the yeast V-ATPase, interacts directly with the Vma1p and Vma13p subunits of the V<sub>1</sub> sector. J. Biol. Chem. **275**: 15449–15457

- 101 Hunt I. E. and Bowman B. J. (1997) The intriguing evolution of the 'b' and 'G' subunits in F-type and V-type ATPases: isolation of the *vma-10* gene from *Neurospora crassa*. *J. Bioenerg. Biomembr.* **29**: 533–540
- 102 Kawano M., Iharashi K., Yamato I. and Kakinuma Y. (2002) Arginine residue at position 573 in *Enterococcus hirae* vacuolar-type ATPase NtpI subunit plays a crucial role in Na<sup>+</sup> translocation. *J. Biol. Chem.* **277**: 24404–24410
- 103 Mandel M., Moriyama Y., Hulmes J. D., Pan Y.-C. E., Nelson H. and Nelson N. (1988) cDNA sequence encoding the 16-kDa proteolipid of chromaffin granules implies gene duplication in the evolution of H<sup>+</sup>-ATPases. *Proc. Natl. Acad. Sci. USA* **85**: 5521–5524
- 104 Hirata R., Graham L. A., Takatsuki A., Stevens T. H. and Anraku Y. (1997) VMA11 and VMA16 encode second and third proteolipid subunits of the *Saccharomyces cerevisiae* vacuolar membrane H<sup>+</sup>-ATPase. *J. Biol. Chem.* **272**: 4795–4803
- 105 Wang S. Y., Moriyama Y., Mandel M., Hulmes J. D., Pan Y. C., Danho W. et al. (1988) Cloning of cDNA encoding a 32-kDa protein. An accessory polypeptide of the H<sup>+</sup>-ATPase from chromaffin granules. *J. Biol. Chem.* **263**: 17638–17642
- 106 Merzendorfer H., Huss M., Schmid R., Harvey W. R. and Wiczorek H. (1999) A novel insect V-ATPase subunit M9.7 is glycosylated extensively. *J. Biol. Chem.* **274**: 17372–17378
- 107 Ludwig J., Kerscher S., Brandt U., Pfeiffer K., Getlawi F., Apps D. K. et al. (1998) Identification and characterization of a novel 9.2-kDa membrane sector-associated protein of vacuolar proton-ATPase from chromaffin granules. *J. Biol. Chem.* **273**: 10939–10947
- 108 Sze H., Schumacher K., Muller M. L., Padmanaban S. and Taiz L. (2002) A simple nomenclature for a complex proton pump: *VHA* genes encode the vacuolar H<sup>+</sup>-ATPase. *Trends Plant Sci.* **7**: 157–161
- 109 Graham L. A., Hill K. J. and Stevens T. H. (1998) Assembly of the yeast vacuolar H<sup>+</sup>-ATPase occurs in the endoplasmic reticulum and requires a Vma12p/Vma22p assembly complex. *J. Cell. Biol.* **142**: 39–49
- 110 Speelmans G., Poolman B., Abee T. and Konings W. N. (1994) The F- or V-type Na<sup>+</sup>-ATPase of the thermophilic bacterium *Clostridium feravidus*. *J. Bacteriol.* **176**: 5160–5162
- 111 Kakinuma Y. and Igarashi K. (1995) Electrogenic Na<sup>+</sup> transport by *Enterococcus hirae* Na<sup>+</sup>-ATPase. *FEBS Lett.* **359**: 255–258
- 112 Krulwich T. A. (1995) Alkaliphiles: 'basic' molecular problems of pH tolerance and bioenergetics. *Mol. Microbiol.* **15**: 403–410
- 113 Van de Vossenberg J. L. C. M., Ubbink-Kok T., Elferink M. G. L., Driessen A. J. M. and Konings W. N. (1995) Ion permeability of the cytoplasmic membrane limits the maximum growth temperature of bacteria and archaea. *Mol. Microbiol.* **18**: 925–932
- 114 Murata T., Takase K., Yamato I., Igarashi K. and Kakinuma Y. (1999) Properties of the V<sub>0</sub>V<sub>1</sub> Na<sup>+</sup>-ATPase from *Enterococcus hirae* and its V<sub>0</sub> moiety. *J. Biochem. (Tokyo)* **125**: 414–421
- 115 Lübbers M., Lünsdorf H. and Schäfer G. (1988) Archaeobacterial ATPase: studies on subunit composition and quaternary structure of the F<sub>1</sub>-analogous ATPase from *Sulfolobus acidocaldarius*. *Biol. Chem. Hoppe Seyler* **369**: 1259–1266
- 116 Wilms R., Freiberg C., Wegerle E., Meier I., Mayer F. and Müller V. (1996) Subunit structure and organization of the genes of the A<sub>1</sub>A<sub>0</sub> ATPase from the archaeon *Methanosarcina mazei* Gö1. *J. Biol. Chem.* **271**: 18843–18852
- 117 Schäfer G. and Meyering-Vos M. (1992) F-Type or V-Type? The chimeric nature of the archaeobacterial ATP synthase. *Biochim. Biophys. Acta* **1101**: 232–235
- 118 Walker J. E., Saraste M., Runswick M. J. and Gay N. J. (1982) Distantly related sequences in the  $\alpha$ - and  $\beta$ -subunits of ATP synthase, myosin, kinases and other ATP-requiring enzymes and a common nucleotide binding fold. *EMBO J.* **1**: 945–951
- 119 Lemker T., Ruppert C., Stoeger H., Wimmers S. and Müller V. (2001) Overproduction of a functional A<sub>1</sub> ATPase from the archaeon *Methanosarcina mazei* Gö1 in *Escherichia coli*. *Eur. J. Biochem.* **268**: 3744–3750
- 120 Stuhmann H. B. (1970) Interpretation of small-angle scattering functions of dilute solutions and gases. A representation of the structures related to a one-particle-scattering function. *Acta. Crystallogr. A* **26**: 297–306
- 121 Coskun Ü., Grüber G., Koch M. H., Godovac-Zimmermann J., Lemker T. and Müller V. (2002) Crosstalk in the A<sub>1</sub>-ATPase from *Methanosarcina mazei* Gö1 due to nucleotide-binding. *J. Biol. Chem.* **279**: 17327–17333
- 122 Deppenmeier U., Johann A., Hartsch T., Merkl R., Schmitz R. A., Martinez-Arias R. et al. (2002) The genome of *Methanosarcina mazei*: evidence for lateral gene transfer between bacteria and archaea. *J. Mol. Microbiol. Biotechnol.* **4**: 453–461
- 123 Galagan J. E., Nusbaum C., Roy A., Endrizzi M. G., Macdonald P., FitzHugh W. et al. (2002) The genome of *Methanosarcina acetivorans* reveals extensive metabolic and physiological diversity. *Genome Res.* **12**: 532–542
- 124 Genbank accession no. NC\_002724
- 125 Deckers-Hebestreit G. and Altendorf K. (1996) The F<sub>0</sub>F<sub>1</sub>-type ATP synthases of bacteria: structure and function of the F<sub>0</sub> complex. *Annu. Rev. Microbiol.* **50**: 791–824
- 126 Fillingame R. H., Jones P. C., Jiang W., Valiyaveetil F. I. and Dmitriev O. Y. (1998) Subunit organization and structure in the F<sub>0</sub> sector of *Escherichia coli* F<sub>1</sub>F<sub>0</sub> ATP synthase. *Biochim. Biophys. Acta* **1365**: 135–142
- 127 Leng X. H., Manolson M. F., Liu Q. and Forgac M. (1996) Site-directed mutagenesis of the 100-kDa subunit (Vph1p) of the yeast vacuolar H<sup>+</sup>-ATPase. *J. Biol. Chem.* **271**: 22487–22493
- 128 Leng X.-H., Manolson M. F. and Forgac M. (1998) Function of the COOH-terminal Domain of Vph1p in activity and assembly of the yeast V-ATPase. *J. Biol. Chem.* **273**: 6717–6723
- 129 Bauerle C., Ho M. N., Lindorfer M. A. and Stevens T. H. (1993) The *Saccharomyces cerevisiae vma-6* gene encodes the 36-kDa subunit of the vacuolar H<sup>+</sup>-ATPase membrane sector. *J. Biol. Chem.* **268**: 12749–12757
- 130 Ihara K., Watanabe S., Sugimura K. and Mukohata Y. (1997) Identification of proteolipid from an extremely halophilic archaeon *Halobacterium salinarum* as an N,N'-dicyclohexylcarbodiimide binding subunit of ATP synthase. *Arch. Biochem. Biophys.* **341**: 267–272
- 131 Inatomi K. I., Maeda M. and Futai M. (1989) Dicyclohexylcarbodiimide-binding protein is a subunit of the *Methanosarcina barkeri* ATPase complex. *Biochem. Biophys. Res. Commun.* **162**: 1585–1590
- 132 Lübbers M. and Schäfer G. (1989) Chemiosmotic energy conservation of the thermoacidophile *Sulfolobus acidocaldarius*: oxidative phosphorylation and the presence of an F<sub>0</sub>-related N,N'-dicyclohexylcarbodiimide-binding proteolipid. *J. Bacteriol.* **171**: 6106–6116
- 133 Steinert K., Wagner V., Kroth-Pancic P. G. and Bickel-Sandkötter S. (1997) Characterization and subunit structure of the ATP synthase of the halophilic archaeon *Haloferax volcanii* and organization of the ATP synthase genes. *J. Biol. Chem.* **272**: 6261–6269
- 134 Ruppert C., Kavermann H., Wimmers S., Schmid R., Kellermann J., Lottspeich F. et al. (1999) The proteolipid of the A<sub>1</sub>A<sub>0</sub> ATP synthase from *Methanococcus jannaschii* has six predicted transmembrane helices but only two proton-translocating carboxyl groups. *J. Biol. Chem.* **274**: 25281–25284
- 135 Ruppert C., Schmid R., Hedderich R. and Müller V. (2001) Selective extraction of subunit D of the Na<sup>+</sup>-translocating methyltransferase and subunit c of the A<sub>1</sub>A<sub>0</sub> ATPase from the



- cytoplasmic membrane of methanogenic archaea by chloroform/methanol and characterization of subunit *c* of *Methanothermobacter thermoautotrophicus* as a 16-kDa proteolipid. FEMS Microbiol. Lett. **195**: 47–51
- 136 Becher B. and Müller V. (1994)  $\Delta\mu_{\text{Na}^+}$  drives the synthesis of ATP via a  $\Delta\mu_{\text{Na}^+}$ -translocating  $\text{F}_1\text{F}_0$ -ATP synthase in membrane vesicles of the archaeon *Methanosarcina mazei* Gö1. J. Bacteriol. **176**: 2543–2550
  - 137 Smigan P., Rusnak P., Greksak M., Zhilina T. N. and Zavarzin G. A. (1992) Mode of sodium ion action on methanogenesis and ATPase of the moderate halophilic methanogenic bacterium *Methanohalophilus halophilus*. FEBS Lett. **300**: 193–196
  - 138 Smigan P., Majernik A. and Greksak M. (1994)  $\text{Na}^+$ -driven ATP synthesis in *Methanobacterium thermoautotrophicum* and its differentiation from  $\text{H}^+$ -driven ATP synthesis by rhodamine 6G. FEBS Lett. **347**: 190–194
  - 139 Smigan P., Majernik A., Polak P., Hapala I. and Greksak M. (1995) The presence of  $\text{H}^+$  and  $\text{Na}^+$ -translocating ATPases in *Methanobacterium thermoautotrophicum* and their possible function under alkaline conditions. FEBS Lett. **371**: 119–122
  - 140 Smith D. R., Doucette-Stamm L. A., Deloughery C., Lee H., Dubois J., Aldredge T. et al. (1997) Complete genome sequence of *Methanobacterium thermoautotrophicum*  $\Delta\text{H}$ : functional analysis and comparative genomics. J. Bacteriol. **179**: 7135–7155
  - 141 Capaldi R. A., Aggeler R., Gogol E. P. and Wilkens S. (1992) Structure of the *Escherichia coli* ATP synthase and role of the  $\gamma$  subunit and  $\epsilon$  subunit in coupling catalytic site and proton channeling functions. J. Bioenerg. Biomembr. **24**: 435–439
  - 142 Capaldi R. A. (1994)  $\text{F}_1$ -ATPase in a spin. Nature Struct. Biology **1**: 660–663
  - 143 Zhou Y. T., Duncan T. M., Bulygin V. V., Hutcheon M. L. and Cross R. L. (1996) ATP hydrolysis by membrane-bound *Escherichia coli*  $\text{F}_0\text{F}_1$  causes rotation of the  $\gamma$  subunit relative to the  $\beta$  subunits. Biochim. Biophys. Acta **1275**: 96–100
  - 144 Sabbert D., Engelbrecht S. and Junge W. (1996) Intersubunit rotation in active  $\text{F}_1$ -ATPase. Nature **381**: 623–625
  - 145 Noji H., Yasuda R., Yoshida M. and Kinosita K. Jr (1997) Direct observation of the rotation of  $\text{F}_1$ -ATPase. Nature **386**: 299–302
  - 146 Yasuda R., Noji H., Yoshida M., Kinosita K. Jr and Itoh H. (2001) Resolution of distinct rotational substeps by submillisecond kinetic analysis of  $\text{F}_1$ -ATPase. Nature **410**: 898–904
  - 147 Capaldi R. A., Schulenberg B., Murray J. and Aggeler R. (2000) Cross-linking and electron microscopy studies of the structure and functioning of the *Escherichia coli* ATP synthase. J. Exp. Biol. **203**: 29–33
  - 148 Sambongi Y., Iko Y., Tanabe M., Omote H., Iwamoto-Kihara A., Ueda I. et al. (1999) Mechanical rotation of the *c* subunit oligomer in ATP synthase ( $\text{F}_0\text{F}_1$ ): direct observation. Science **286**: 1722–1724
  - 149 Pänke O., Gumbiowski K., Junge W. and Engelbrecht S. (2000)  $\text{F}_1$ -ATPase: specific observation of the rotating *c* subunit oligomer of  $\text{EF}_0\text{EF}_1$ . FEBS Lett. **472**: 34–38
  - 150 Kaim G., Prummer M., Sick B., Zumofen G., Renn A., Wild U. P. et al. (2002) Coupled rotation within single  $\text{F}_0\text{F}_1$  enzyme complexes during ATP synthesis or hydrolysis. FEBS Lett. **525**: 156–163
  - 151 Kaim G., Matthey U. and Dimroth P. (1998) Model of interaction of the single *a* subunit with the multimeric *c* subunits during the translocation of the coupling ions by  $\text{F}_1\text{F}_0$  ATPases. EMBO J. **17**: 688–695
  - 152 Dimroth P., Kaim G. and Matthey U. (1998) The motor of the ATP synthase. Biochim. Biophys. Acta **1365**: 87–92
  - 153 Kaim G. and Dimroth P. (1998) A triple mutation in the *a* subunit of the *Escherichia coli*/*Propionigenium modestum*  $\text{F}_1\text{F}_0$  ATPase hybrid causes a switch from  $\text{Na}^+$  stimulation to  $\text{Na}^+$  inhibition. Biochemistry **37**: 4626–4634
  - 154 Junge W., Pänke O., Cherepanov D. A., Gumbiowski K., Müller M. and Engelbrecht S. (2001) Inter-subunit rotation and elastic power transmission in  $\text{F}_0\text{F}_1$ -ATPase. FEBS Lett. **504**: 152–160
  - 155 Capaldi R. A. and Aggeler R. (2002) Mechanism of the  $\text{F}_1\text{F}_0$ -type ATP synthase, a biological rotary motor. Trends Biochem. Sci. **27**: 154–160
  - 156 Werner-Grüne S., Gunkel D., Schumann J. and Strotmann H. (1994) Insertion of a 'chloroplast-like' regulatory segment responsible for thiol modulation into  $\gamma$ -subunit of  $\text{F}_0\text{F}_1$ -ATPase of the cyanobacterium *Synechocystis* 6803 by mutagenesis of *atpC*. Mol. Gen. Genet. **244**: 144–150
  - 157 Hirata T., Nakamura N., Omote H., Wada Y. and Futai M. (2000) Regulation and reversibility of vacuolar  $\text{H}^+$ -ATPase. J. Biol. Chem. **275**: 386–389
  - 158 Schemidt R. A., Qu J., Williams J. R. and Brusilow W. S. (1998) Effects of carbon source on expression of  $\text{F}_0$  genes and on the stoichiometry of the *c* subunit in the  $\text{F}_1\text{F}_0$  ATPase of *Escherichia coli*. J. Bacteriol. **180**: 3205–3208
  - 159 Gogarten J. P. and Taiz L. (1992) Evolution of proton pumping ATPases – rooting the tree of life. Photosynth. Res. **33**: 137–146
  - 160 Nelson N. and Taiz L. (1989) The evolution of  $\text{H}^+$ -ATPases. Trends Biochem. Sci. **14**: 113–116
  - 161 Olendzenski L., Hilario E. and Gogarten J. P. 1998. Horizontal gene transfer and fusing lines of descent: the Archaeobacteria – a chimera? In: Horizontal Gene Transfer, p. 349–363. Syvanen K. and Kado C. I. (eds), Chapman and Hall, New York
  - 162 Friedrich A., Hartsch T. and Averhoff B. (2001) Natural transformation in mesophilic and thermophilic bacteria: identification and characterization of novel, closely related competence genes in *Acinetobacter* spec. strain BD413 and *Thermus thermophilus* HB27. Appl. Environ. Microbiol. **67**: 3140–3148
  - 163 Friedrich A., Prust C., Hartsch T., Henne A. and Averhoff B. (2002) Molecular analyses of the natural transformation machinery and identification of pilus structures in the extremely thermophilic bacterium *Thermus thermophilus* strain HB27. Appl. Environ. Microbiol. **68**: 745–755
  - 164 Kakinuma Y., Yamato I. and Murata T. (1999) Structure and function of vacuolar  $\text{Na}^+$ -translocating ATPase in *Enterococcus hirae*. J. Bioenerg. Biomembr. **31**: 7–14
  - 165 Nelson N. (1992) Evolution of organellar proton-ATPases. Biochim. Biophys. Acta **1100**: 109–124
  - 166 Klenk H. P., Clayton R. A., Tomb J. F., White O., Nelson K. E., Ketchum K. A. et al. (1997) The complete genome sequence of the hyperthermophilic, sulphate-reducing archaeon *Archaeoglobus fulgidus*. Nature **390**: 364–370
  - 167 Kawarabayashi Y., Sawada M., Horikawa H., Haikawa Y., Hino Y., Yamamoto S. et al. (1998) Complete sequence and gene organization of the genome of a hyperthermophilic archaeobacterium, *Pyrococcus horikoshii* OT3. DNA Res. **5**: 55–76
  - 168 Adams M. W. W. (1994) Biochemical diversity among sulfur-dependent, hyperthermophilic microorganisms. FEMS Microbiol. Rev. **15**: 261–277
  - 169 Cross R. L. and Taiz L. (1990) Gene duplication as a means for altering  $\text{H}^+$ /ATP ratios during the evolution of  $\text{F}_0\text{F}_1$  ATPases and synthases. FEBS Lett. **259**: 2222–2229
  - 170 Jones P. C. and Fillingame R. H. (1998) Genetic fusions of subunit *c* in the  $\text{F}_0$  sector of  $\text{H}^+$ -transporting ATP synthase. Functional dimers and trimers and determination of stoichiometry by cross-linking analysis. J. Biol. Chem. **273**: 29701–29705
  - 171 McCarthy J. E., Schairer H. U. and Sebald W. (1985) Translational initiation frequency of *atp* genes from *Escherichia coli*: identification of an intercistronic sequence that enhances translation. EMBO J. **4**: 519–526



- 172 McCarthy J. E., Gerstel B., Surin B., Wiedemann U. and Ziemke P. (1991) Differential gene expression from the *Escherichia coli atp* operon mediated by segmental differences in mRNA stability. *Mol. Microbiol.* **10**: 2447–2258
- 173 Ruppert C., Wimmers S., Lemker T. and Müller V. (1998) The  $A_1A_0$  ATPase from *Methanosarcina mazei*: cloning of the 5' end of the *aha* operon encoding the membrane domain and expression of the proteolipid in a membrane-bound form in *Escherichia coli*. *J. Bacteriol.* **180**: 3448–3452
- 174 Bernstein F. C., Koetzle T. F., Williams G. J., Meyer E. F. Jr, Brice M. D., Rodgers J. R. et al. (1977) The Protein Data Bank: a computer-based archival file for macromolecular structures. *J. Mol. Biol.* **112**: 535–542
- 175 Girvin M. E., Rastogi V. K., Abildgaard F., Markley J. L. and Fillingame R. H. (1998) Solution structure of the transmembrane  $H^+$ -transporting subunit *c* of the  $F_1F_0$  ATP synthase. *Biochemistry* **37**: 8817–8824



To access this journal online:  
<http://www.birkhauser.ch>

---